



Stock Assessment of the dolphinfish (*Coryphaena hippurus*) in the South-East Pacific Ocean (1988-2019)

AUTHORS

Rubén H. Roa-Ureta¹
Gersson Román Amancio²
Pablo Marín Abanto²
Iván Guevara Izquierdo²
Ana Alegre Norza Sior²
Esteban Elías³,
Manuel Peralta³

1 Consultant in Statistical Modelling, Marine Ecology and Fisheries

2 Instituto del Mar del Perú (IMARPE)

3 Instituto Público de Investigación de Acuicultura y Pesca (IPIAP)

July 6, 2022

Acknowledgements.



The findings, interpretations, and conclusions expressed in this work do not necessarily reflect the views of Sustainable Fisheries Partnership. The Sustainable Fisheries Partnership does not guarantee the accuracy of the data included in this work.

Contents

1	Introduction	1
2	Materials and Methods	4
2.1	Data	5
2.2	Generalized depletion models	8
2.3	Population dynamics models	12
3	Results	15
3.1	Generalized depletion models	15
3.2	Population dynamics models	26
4	Discussion	29
5	Conclusions	31
6	Management Advice	32
	List of Figures	I
	List of Tables	II
	References	III

Executive Summary

A database of fishing effort, catches and mean fish weight by two Peruvian fleets and two Ecuadorian fleets since January 2004 and up to December 2019, at monthly time steps, was built to conduct a stock assessment of the dolphinfish stock in the South-East Pacific. A hierarchical statistical inference framework connected a multi-annual multi-fleet generalized depletion model using catch, effort and mean weight data, to a surplus production model of the Pella-Tomlinson type fitted to annual biomass predictions of the depletion model. To fit the surplus production model a further database of total annual catch back in time to 1988 was created from FAO landings statistics of fleets from both countries. The biomass dynamics in the surplus production model included environmentally-driven forcing that changed the values of parameters in the model during warm, El Niño Southern Oscillation (ENSO) years versus during cold, normal periods of the environmental cycle. The model was written in R (depletion model) and ADMB (surplus production model).

Among 36 variants of the depletion model, differing in the timing of annual recruitment pulses, the likelihood model for the data, and the numerical method for optimization, the best model estimated very high natural mortality rates (0.339 per month) with good statistical precision (5% CV). Annual recruitment pulses to the whole region and the four fleets varied from a few million to a few hundred million fish, and catches were generally proportional to fishing effort and hyper-stable to abundance. Aggregate and instantaneous exploitation rates (as well as fishing mortality) were well within sustainable levels for the whole length of the time series 2004-2019.

Analysis of NOAA indicators of ENSO determined the existence of a cycle of four periods. A cold, normal period between 1988 and 1996, a warm, ENSO period between 1997 and 2002, a further cold period between 2003 and 2004, and a final warm period between 2014 and 2019. This environmental cycle caused a biomass dynamics in the stock that changed the intrinsic population growth rate from cold to warm periods, with the latter having higher intrinsic population growth rate and no change in other parameters of the biomass dynamics.

The environmental cycle produced changing annual sustainable harvest rates, with the cold part of the cycle yielding higher harvest rates. In both phases of the environmental cycle, the annual catches aggregated across all four fleets were well below sustainable harvest rates. This further confirms that the fishing of the dolphinfish stock in the South East Pacific is being conducted within sustainable limits.

During warm, ENSO years the stock experiences much wider fluctuations than during cold, normal periods. This shows that the environmental cycle is superimposed onto intrinsic population fluctuations that get triggered to a higher level whenever the region enters the warm part of the cycle. This further highlights the importance of ecosystem considerations for management oriented to sustainability.

1 Introduction

The dolphinfish is a large epipelagic and migratory species from tropical and subtropical oceans that has been fished in all regions where it is found since ancient times [1]. The species is captured in large volumes (thousand tonnes) in the Western Indian Ocean (Iran and Pakistan), North-West Pacific (Taiwan), Western Central Pacific (Indonesia), Western Mediterranean (Italy, Tunisia, Spain and Malta) and the South-East Pacific (Peru and Ecuador) [2]. It is also captured in the Caribbean [3] and Florida and North Carolina, U.S.A [4]. The largest landings occur in the South-East Pacific and in particular the Peruvian fishery is the largest dolphinfish fishery in the world [2]. In the Exclusive Economic Zones (EEZ) of both Peru (815,915 km²) and Ecuador (1,077,231 km², including the Galapagos archipelago) (Fig. 1) the dolphinfish is an important fishery resource captured by local artisanal fleets using drifting longlines.

Although the species sustains large total landings worldwide, well exceeding 100 thousand tonnes in the last decade (Fig. 2, top panel), the stock assessment of local stocks remains difficult due to scarcity of data and fast population dynamics. Nevertheless, several authors have attempted various stock assessment methods in their areas of operation. Benjamin and Kurup [5] applied yield per recruit and virtual population formulas to the stock fished off the South-West coast of India to conclude that the stock is fished within sustainable levels. Baset *et. al.* [6] applied non-equilibrium surplus production models to the dolphinfish catch records and (apparently un-standardized) annual CPUE indices of abundance from the Pakistan fishery using the CEDDA stock assessment package [7]. This method depends on an assumption of depletion degree (0 to 90%) at the start of the time series and in Baset *et. al.* application, results varied widely depending on the value assumed, from MSY equal to a few thousands tonnes at low starting depletion degree values to a few million tonnes at high starting depletion degree values. Nevertheless, the authors concluded that the stock was being overfished due to catches larger than the most reasonable MSY estimates. Aires-da-Silva *et. al.* [8] conducted an exploratory stock assessment of the stock fished in the South-East Pacific, namely within the Peruvian and Ecuadorian EEZs (Fig. 1), using a length-structured model with monthly time steps in the Stock Synthesis package [9]. Although this assessment was technically more advanced than the assessments cited above and it could be considered as data-rich and conventional, it included several parameters fixed at arbitrary values chosen by the analysts, such as the natural mortality rate, the steepness of the stock-recruitment relationship, and other parameters that resulted in giving more weight to specific pieces of data. The authors conclude that recent catches (up to June 2015) were close to the estimated MSY but that the fishing mortality that yields the MSY is undefined due to a flat yield-per-recruit curve. Finally, in the Mediterranean Sea the General Fisheries Commission for the Mediterranean (GFCM) of the Food and Agriculture Organization of the United Nations (FAO) has been working on the assessment and management of the dolphinfish stock that migrates into the Mediterranean every summer and is fished there by artisanal fleets from several countries. In 2019 the working group assigned with the assessment of the stock recommended the implementation of generalized depletion models [10] and published a substantial review of dolphinfish biology and its fisheries [11].

Subsequently, the working group developed a customized version of generalized depletion models [12, 13, 14, 15, 16, 17] in software CatDyn [18] and applied it to the data from five fleets operating in the Western Mediterranean Sea [19, 20]. This was reported as the first stock assessment that succeeded in yielding management-useful results. It showed that the stock was being fished in sustainable manner in the region and developed biological reference points connected to the instantaneous exploitation rates [20].



Figure 1: Map of Peruvian and Ecuadorian EEZs where the fishery is conducted.

The dolphinfish Peruvian and Ecuadorian fisheries are clearly the largest dolphinfish fisheries worldwide, accounting for nearly 50% of worldwide dolphinfish catches since 2013 (Fig. 2, top panel). They have been described as data poor fisheries and the stock dynamics as highly productive, variable and fast, making the stock assessment by conventional methods difficult to apply [21].

In this work, we have adapted the multi-annual generalized depletion model built for the assessment of the dolphinfish stock in the Mediterranean Sea [20] to the situation of the fishery in the South-East Pacific, namely Peruvian and Ecuadorian EEZs. The main changes in the depletion model developed for the South-East Pacific as compared to the Mediterranean were that the number of fleets changed from five to four and the time series

extended from January 2004 to December 2019.

Building upon the work done in the Mediterranean, here we further use results of the depletion model in a hierarchical inference statistical framework to fit an environmentally-driven non-equilibrium surplus production model of the Pella-Tomlinson type. Parameters of these model are time-varying following well-known environmental cycles of warming and cooling from the El Niño Southern Oscillation [22]. We present results useful for management in the form of instantaneous and aggregate exploitation rates, biomass levels that support sustainable exploitation, and catch rates that take into account the productive capacity of the stock.

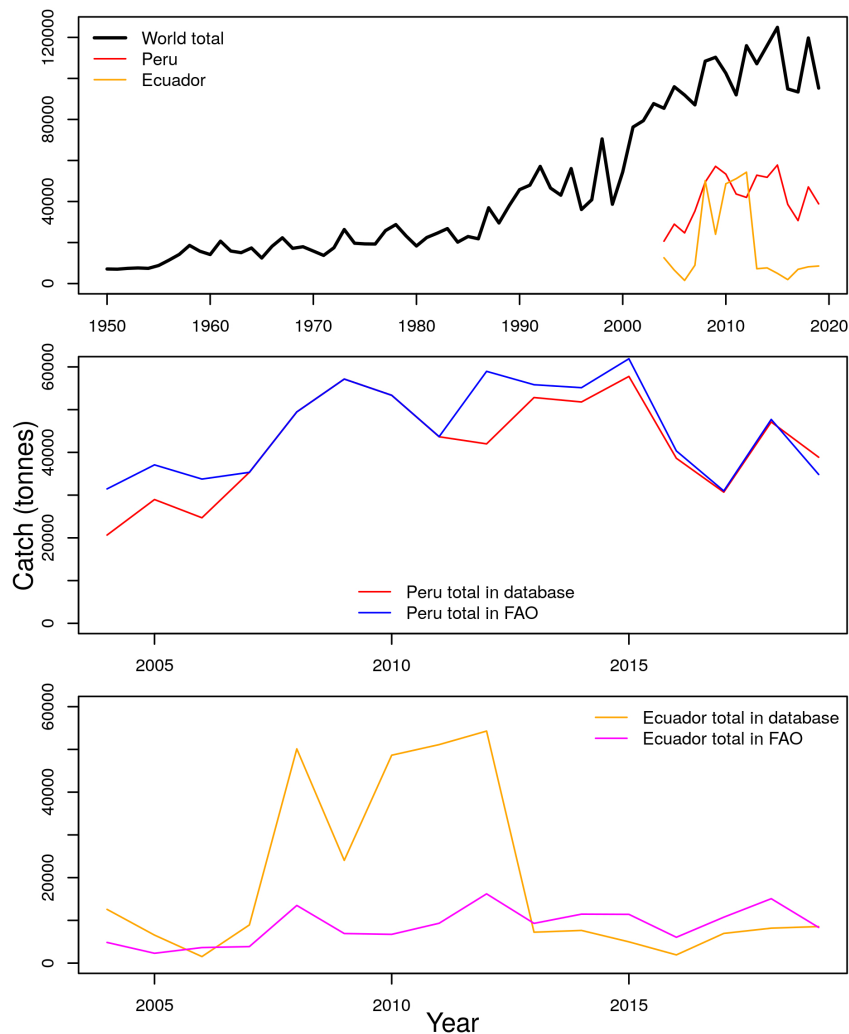


Figure 2: World and country landings and contrast between catch data in the stock assessment database and in FAO databases [23] for the two countries.

2 Materials and Methods

The general approach to the stock assessment of the dolphinfish stock in the South-East Pacific (Peruvian and Ecuadorian EEZs) is portrayed in schematic fashion in Fig. 3 and consists of (1) developing and curating a database of monthly total catch, monthly total effort, and sampled mean monthly weight from four fleets (two artisanal fleets in each country) for the period of January 2004 to December 2019, (2) fitting several variants of generalized depletion models and selection of the best variants in terms of numerical, statistical and biological criteria, and (3) use output from the best generalized depletion model to fit an environmentally-driven surplus production model. Steps (2) and (3) yield several management-useful quantities that constitute potential biological reference points (BRPs).

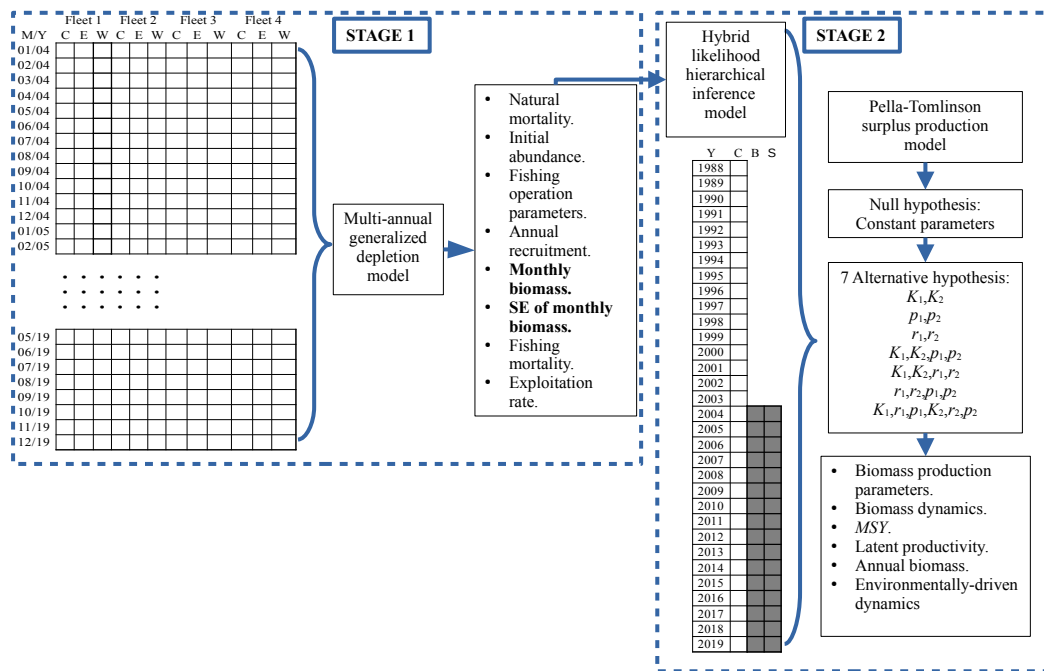


Figure 3: Schematic representation of the stock assessment modelling approach. At Stage 1, catch (C), fishing effort (E) and mean weight in the catch (W) data at monthly time steps from Jan. 2004 to Dec. 2019 is used to fit a multi-annual four-fleets generalized depletion model. From the output of this model, annual biomass estimates (B, 2004 to 2019) and their standard errors (S) in addition to total annual catch (C, 1988 to 2019) are used in Stage 2 to fit a time-varying parameters Pella-Tomlinson model. Eight alternative hypotheses are tested: constant parameters (null hypothesis) and seven alternative hypotheses where parameters K , p and r vary singly or in pairs or trios from warm to cold water regimes.

2.1 Data

The database described in this subsection was compiled as a spreadsheet and then it was imported to the R system of statistical programming [24, 25], where it has been stored as a binary repository.

The data consisted of monthly total catch, monthly total effort, and sampled mean monthly weight or sample mean length from the Peruvian artisanal longline fleet, which operates in coastal and oceanic waters in the Peruvian EEZ, the Peruvian fibreglass boats fleet that operates in coastal waters in the Peruvian EEZ, the Ecuadorian artisanal fleet operating in coastal and oceanic waters in the Ecuadorian EEZ, and the Ecuadorian fibreglass boats fleet that operates in coastal waters in the Ecuadorian EEZ. The Peruvian part of the database contained sampled mean weight in the catch that could not be split between the artisanal and fibreglass fleets so it was considered as valid for both Peruvian fleets. The Ecuadorian part of the database contained sampled mean length in the catch that also could not be split between the artisanal and fibreglass fleets so it was considered as valid for both Ecuadorian fleets. The period covered was January 2004 to December 2019. When aggregated to the annual time step and across both types of fleet per country, the Peruvian catch data shows substantial agreement with the data reported to FAO (Fig. 2, middle panel) while the Ecuadorian catch data shows agreement with that reported to FAO between 2004 and 2007 and between 2013 and 2019, with substantial differences between 2008 and 2012 (Fig. 2, bottom panel). At this point we considered the new database compiled for Ecuador as more accurate than the totals reported to FAO, thus the stock assessment was conducted using the newly compiled database, which included a large increase in Ecuadorian catches between 2008 and 2012.

The original database compiled for stock assessment had missing data. The pattern of missing data is shown in Fig. 4. Over 60% of mean weight data from Peruvian fleets is missing, followed by fishing effort by the Ecuadorian fibreglass fleet at over 40%, and the last significant amount of missing data being the sample mean length data of Ecuadorian fleets (Fig. 4, left panel). Most months (60) are missing mean weight in the catch of the Peruvian fleets and fishing effort by the Ecuadorian fibreglass fleet, with another large number (34) just missing mean length in the catch of Ecuadorian fleets (Fig. 4, right panel).

To replace all missing data with realistic imputed values, a standard statistical methodology for the imputation of indispensable missing data was implemented: predictive mean matching in R package mice [26]. This method consists of the following steps

- Carry out multiple linear regressions on the available data to predict the missing data. We had five completely observed variables (year, month, total catch of the Peruvian artisanal fleet, total effort of the Ecuadorian fibreglass fleet, and total catch of the Peruvian fibreglass fleet) and three nearly completely observed variables (total catch of the Ecuadorian artisanal fleet, total fishing effort of the Ecuadorian artisanal fleet, total fishing effort of the Peruvian artisanal fleet), so predictions are expected to be accurate. This produced slope estimates and their covariance matrix.
- Random sample slope values from the multivariate normal distribution created by slope estimates and their covariance matrix. By including the covariance matrix this step

produces natural variability so predictions of missing data would look more realistic.

- Use the randomized slope values and observed data to predict the whole set of data, including in months in which true values were observed and were missing.
- For missing data, find the set of observed data that most closely resembles the same data in the missing effort months.
- Take one random value for each predicted datum from the set of predicted data that belongs with the observed data that most closely resembles the current missing data.

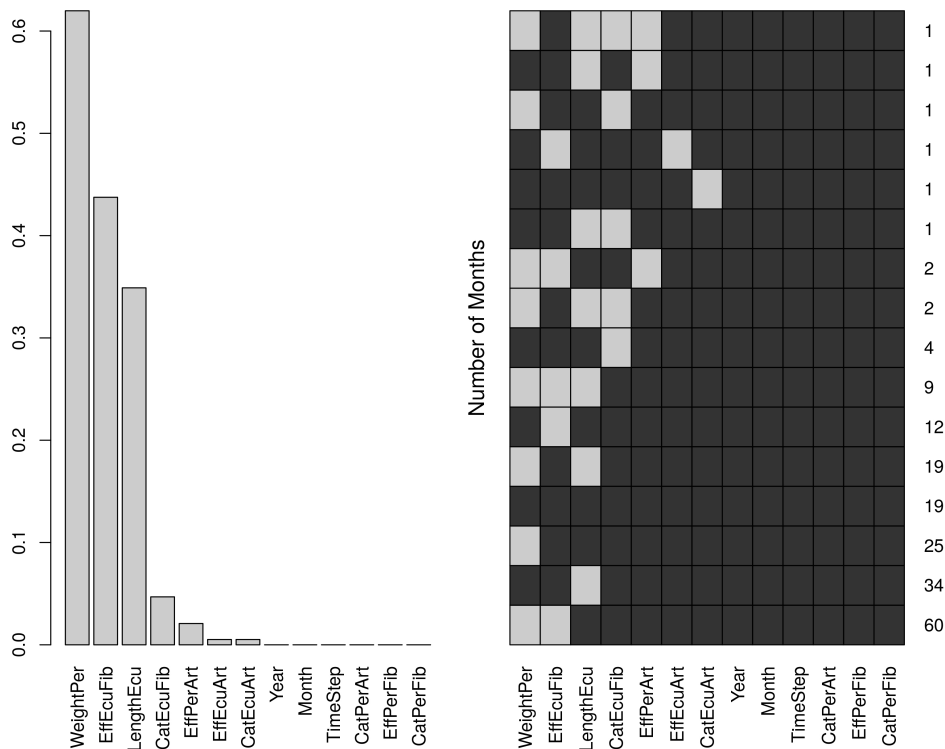


Figure 4: Pattern of missing data in the original database compiled for stock assessment of the stock of dolphinfish in the South-Eastern Pacific (Peru and Ecuador). The left panel is a histogram of months with missing data per variable. The right panel is the number of months missing data at particular combinations of the variables. The variables are *WeightPer*: mean weight in Peruvian catches; *EffEcuFib*: total fishing effort in the Ecuadorian fibreglass fleet; *LengthEcu*: mean length in Ecuadorian catches; *CatEcuFib*: total catch in the Ecuadorian fibreglass fleet; *EffPerArt*: total fishing effort in the Peruvian artisanal fleet; *EffEcuArt*: total fishing effort in the Ecuadorian artisanal fleet; *CatEcuArt*: total catch in the Ecuadorian artisanal fleet; *CatPerArt*: total catch in the Peruvian artisanal fleet; *EffPerFib*: total fishing effort in the Peruvian fibreglass fleet; and *CatPerFib*: total catch in the Peruvian fibreglass fleet.

In this manner we assembled a complete database for stock assessment. Finally, mean length data in the catch of Ecuadorian fleets was used to calculate mean weight in the catch of those fleets. For this we used the length-weight relationship in Zúñiga-Flores [27], determined from dolphinfish samples of fork length and weight taken in Baja California, Mexico. The resulting effort and catch data is shown in Fig. 5. The best effort-catch relationship is observed in the Peruvian fibreglass fleet, followed by Peruvian artisanal fleet. Ecuadorian data show over-dispersion (fibreglass) and weak determination of catch from effort for a wide range of effort (artisanal).

Generalized depletion models predict the catch by time step in numbers, not in weight. Therefore the monthly catch recorded in weight in the database needed to be transformed to numbers by using the the time series of mean weight. The complete mean weight time series is shown in Fig. 6. There is ample intra-annual variability in both time series, as expected given the very fast growth rate that characterizes the species [11]. Ecuadorian fleets seem to catch larger fish than Peruvian fleets.

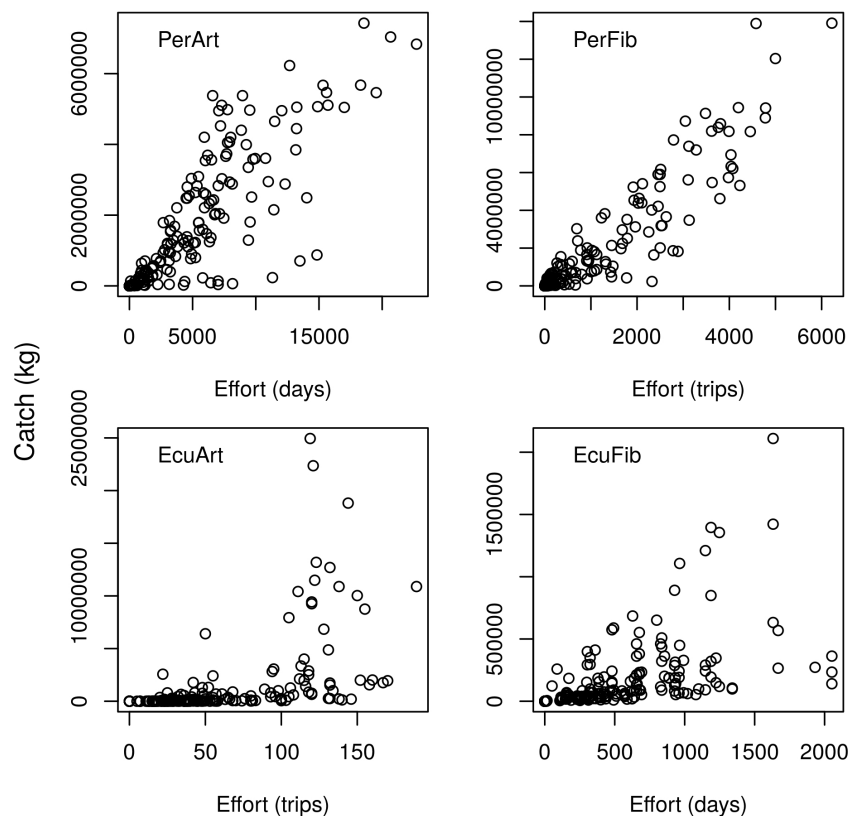


Figure 5: Effort and catch data in four fleets operating in the South-East Pacific (Peru and Ecuador). PerArt: Peruvian artisanal; PerFib: Peruvian fibreglass; EcuArt: Ecuadorian artisanal; EcuFib: Ecuadorian fibreglass.

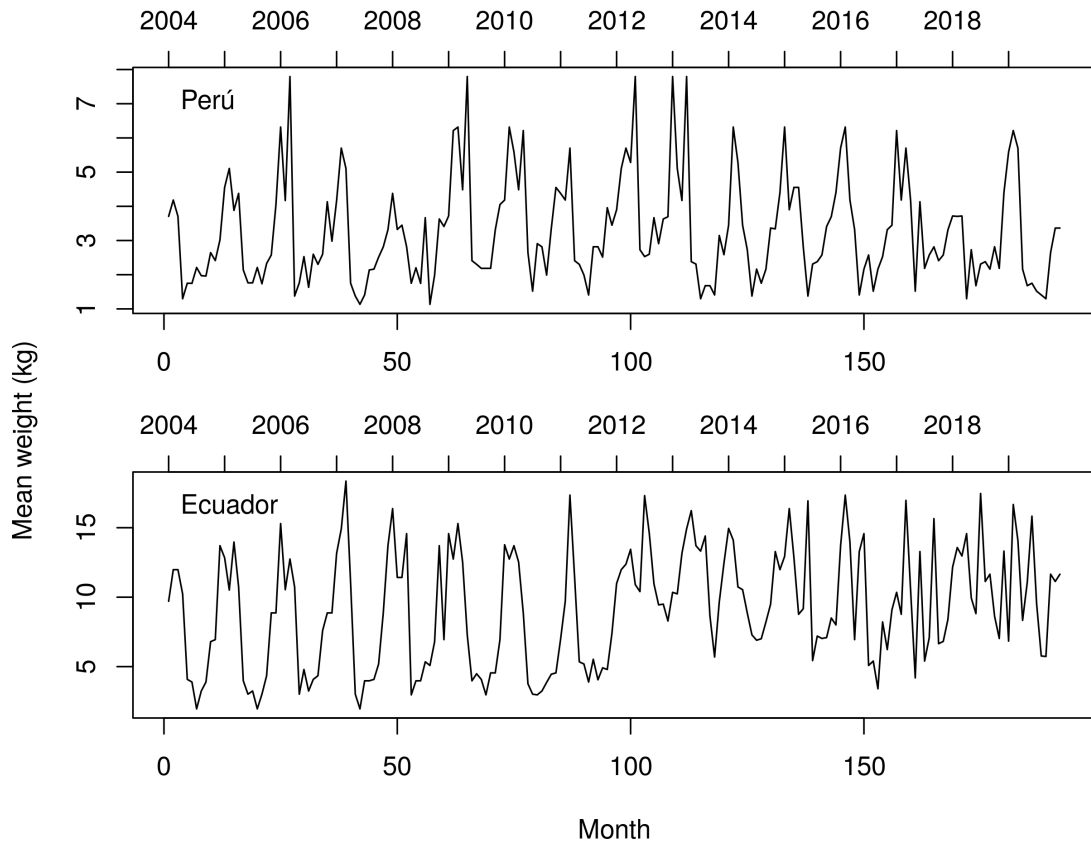


Figure 6: Mean weight time series used to transform catch in weight to catch in numbers.

2.2 Generalized depletion models

The stock assessment methodology employed here has been described in several recent scientific articles [12, 28, 13, 29, 14, 15, 16, 17, 18, 30, 31, 20]. The model developed for this case is an extension of multi-annual generalized depletion models [13, 16, 31]. These models run at monthly time steps and analyze the data from several annual fishing season simultaneously. The models contain parameters for initial abundance, the average natural mortality rate over the period of years covered by the time series of data, the magnitude of annual recruitment pulses to each fleet (i.e. there is a total number of number of years \times number of fleets, $16 \times 4 = 64$ recruitment parameters) and three fishing operational parameters that are fleet-specific (i.e. $3 \times 4 = 12$ fishing operational parameters). These models are fully mechanistic models in which all parameters are estimated freely, not fixing any parameter at arbitrary values. The generalized depletion model specific to this case has 78 parameters to estimate and is of the form:

$$\begin{aligned}
C_t &= k_1 E_{1,t}^{\alpha_1} N_t^{\beta_1} + k_2 E_{2,t}^{\alpha_2} N_t^{\beta_2} + k_3 E_{3,t}^{\alpha_3} N_t^{\beta_3} + k_4 E_{4,t}^{\alpha_4} N_t^{\beta_4} \\
C_t &= k_1 E_{1,t}^{\alpha_1} e^{M/2} \left(N_0 e^{-Mt} - e^{M/2} \left[\sum_{i=1}^{i=t-1} C_{1,i} e^{-M(t-i-1)} \right] + \sum_{j=1}^{j=16} I_{1,j} R_{1,j} e^{-M(t-\tau_{1,j})} \right)^{\beta_1} + \\
& k_2 E_{2,t}^{\alpha_2} e^{M/2} \left(N_0 e^{-Mt} - e^{M/2} \left[\sum_{i=1}^{i=t-1} C_{2,i} e^{-M(t-i-1)} \right] + \sum_{j=1}^{j=16} I_{2,j} R_{2,j} e^{-M(t-\tau_{2,j})} \right)^{\beta_2} + \\
& k_3 E_{3,t}^{\alpha_3} e^{M/2} \left(N_0 e^{-Mt} - e^{M/2} \left[\sum_{i=1}^{i=t-1} C_{3,i} e^{-M(t-i-1)} \right] + \sum_{j=1}^{j=16} I_{3,j} R_{3,j} e^{-M(t-\tau_{3,j})} \right)^{\beta_3} + \\
& k_4 E_{4,t}^{\alpha_4} e^{M/2} \left(N_0 e^{-Mt} - e^{M/2} \left[\sum_{i=1}^{i=t-1} C_{4,i} e^{-M(t-i-1)} \right] + \sum_{j=1}^{j=16} I_{4,j} R_{4,j} e^{-M(t-\tau_{4,j})} \right)^{\beta_4} \quad (1)
\end{aligned}$$

where:

- t is the time step (month),
- C is the unobserved, true catch in numbers,
- k is a proportionality constant, the scaling, that corresponds to the catch taken by a unit of effort and a unit of abundance, usually in the order of 10^{-4} to 10^{-8} ,
- E is the observed fishing effort in hours,
- N is the latent stock abundance in numbers,
- α is a dimensionless modulator of effort as a predictor of catch, called the effort response,
- β is a dimensionless modulator of abundance as a predictor of catch, called the abundance response,
- M is the natural mortality rate with units of month^{-1} ,
- m equals $e^{M/2}$,
- N_0 is the initial abundance, the abundance at month before the first month in the effort and catch time series (December 2014),
- i is an index that runs over previous time steps and up to the current time step (t),
- R are the magnitudes of annual pulses of recruitment of dolphinfish that grow to the size retained by the fishers to each of the fleets,

- I is an indicator variables that evaluates to 0 before the recruitment pulse and to 1 during and after the recruitment pulse,
- 16 is the number of recruitment pulses, one for each year, happening at a specific month each year, with j being the counter that runs from 1 to 16, and
- τ is the specific month at which each recruitment pulse happens.

Parameters M , N_0 , and the 64 recruitment magnitudes are stock abundance parameters while k , α and β are fishing operational parameters. The conceptual basis of this model is presented in the first line of Eq. 1. The true catch at each month C is the product of the fishing effort E expended that month and the latent stock abundance that month, and this product is scaled by the scaling k . The model allows for zero catches in some months either because there was zero effort or there was zero abundance. The model is a mechanistic model because it ascertains a specific cause-effect: effort and abundance are necessary causes and the catch is the effect. In the second line of Eq. 1 the model is completed by using Pope's recursive expansion plus the effect of recruitment pulses to fully specify the mathematical form of C_t .

Parameters α and β are power modulators of the effect of both predictors on the true catch that enable discovery of nonlinear effects. Specifically, the effort response α modulates the continuum of effort saturation ($\alpha < 1$) \leftrightarrow proportionality ($\alpha \approx 1$) \leftrightarrow synergy ($\alpha > 1$) and the abundance response β modulates the continuum of abundance hyperstability ($\beta < 1$) \leftrightarrow proportionality ($\beta \approx 1$) \leftrightarrow hyperdepletion ($\beta > 1$). Effort saturation occurs when a fishing gear becomes full quickly so any additional unit of effort does not produce a proportional increase in catch, while the opposite effect, effort synergy occurs when additional units of effort produce more additional catch than expected under proportionality. Abundance hyperstability happens when declining stock abundance is not reflected in less catch, while abundance hyperdepletion happens when the catch decreases faster than the decline in the stock. Effort saturation may happen when fishing gears are small, for instance a crab trap may not catch more crabs even though it stays longer time because it is full of crabs. Effort synergy happens when fishing gears work better when there are more of them, for instance traps that have baits, which when larger in number, create a greater area of attraction to the target stock. Hyperstability is common in fisheries that capture aggregations of fish since the catch may remain high even when aggregations are being depleted because the fish will aggregate again as the gear thins the aggregation making it possible for the fishers to continue having high catches as abundance decreases. Hyperdepletion happens when fishing gears scare the fish away so it seems from the fishers point of view that the stock is being depleted while the reality is that the stock is being dispersed.

In the model, total recruitment to the stock in any year is the sum of the recruitments to each fleet: $R_y = R_{1,y} + R_{2,y} + R_{3,y} + R_{4,y}$, where y is the year, and the concept behind this additivity is that each fleet 'sees' a part of the total recruitment.

Using the catch in numbers and effort time series for sufficiently long time series (i.e. when the number of time steps is several times the number of parameters) allows simultaneous estimation of N_0 , M , k , the recruitment pulses R_j , α , and β . The timing τ_j of recruitment pulses are estimated by fitting models with varying configurations of τ_j and then selecting

the configuration best supported by the data. These configurations are defined by a range of possible integer values for τ_j , that translate into a range of time steps across which recruitment might take place. To identify these parameters, the model is run with alternative values. The values that maximize the likelihood (when the likelihood model is comparable across model fits) and/or are best according to other criteria (see below), are chosen. In this work models were fitted with 3 options for the timing of these pulses τ_j . Good candidate values for the timings were determined by examination of the non-parametric catch spike statistic, defined as [13],

$$Spike_t = 10 \left(\frac{\chi_t}{\max(\chi_t)} - \frac{E_t}{\max(E_t)} \right) \quad (2)$$

where χ is the observed catch. It highlights time steps with excessively high catch for the effort at that time step. Thus large positive spikes suggest recruitment pulses. See Fig. 3 in Roa-Ureta et al. [28] for a graphical demonstration of the use the spike statistic. The use of the non-parametric statistic is not arbitrary because the best configuration is selected as the model with the configuration that maximizes the likelihood function.

The model in Eq. 1 describes the deterministic process that generates the expected catch under the model. The statistical framework is completed by taking the four observed catch time series as random variables whose mean time series is Eq. 1 with realized time series coming from any of a number of distributions. These distributions define the likelihood function that is to be maximized. Among these, the normal and lognormal distribution have simple formulas for the adjusted profile likelihood, an approximation that eliminates the dispersion parameter from the estimation problem. Models were fitted with the adjusted profile normal, adjusted profile lognormal, exact normal and exact lognormal likelihoods. Formulas used are all listed in [16, Table 2].

Generalized depletion models were fitted using a customized version of R package CatDyn [18]. All parameters are free parameters to be estimated, none of them is fixed at arbitrary values. The latest version also estimates fishing mortality per time step by using a numerical resolution (R function *uniroot*) of the Baranov equation from estimates of abundance, natural mortality and (observed and estimated) catch per time step. CatDyn depends on package *optimx* [32], which makes it simple to call several numerical optimization routines as alternatives to minimise the negative log-likelihood. The *spg* and the *CG* numerical routines were employed because these have yielded reliable results in previous applications [12, 28, 13, 29, 14, 15, 16, 17, 18, 30]. The combination of options for timing of those pulses, likelihood function, and numerical optimization routine led to fitting 36 alternative model variants for the effort and catch (in numbers) time series. We selected the best model by employing the following numerical, biological and statistical criteria. Firstly, all fits returning a numerical gradient higher than 1 for parameters determining the estimation of abundance and biomass (M, N_0 , and the 64 recruitment magnitudes) were eliminated. This is a commonly employed criterion in stock assessment [33, 34, 35, 36]. Secondly, variants yielding unrealistic values of the natural mortality rate (i.e. less than 0.1 per month) given the known lifespan of the dolphinfish were also excluded). Thirdly, from the short list of model fits, the best fit was selected as the one with the lowest standard errors and with the

histogram of correlation coefficients between parameter estimates more concentrated around zero. The histogram of correlation coefficients presents the distribution of pairwise correlations between parameter estimates. It is desirable that these correlations are as far away from 1 or -1 as possible because that means that each parameter was a necessary component of the model. Information theory model selection methods such as the Akaike Information Criterion (AIC) are also useful at this stage when comparing models run with the same likelihood or approximation to the likelihood.

Directly from results of fitting generalized depletion model, it is possible to calculate two measures of exploitation rate: aggregated (catch in numbers over abundance) and instantaneous ($F/(F + M) = F/Z$), where F is the fishing mortality rate. F is calculated in the software by resolving F from knowledge of catch (in numbers), abundance and natural mortality M using Baranov's catch equation:

$$C_{t,f} = N_t \frac{F_{t,f}}{F_{t,f} + M} (1 - e^{-(F_{t,f} + M)t}) \quad (3)$$

Both measures of exploitation rate can be used directly for management but particularly for the instantaneous exploitation rate, there is a study demonstrating that for stocks with the life history of small pelagic fish instantaneous exploitation rates less than 40% maintain a stable and sustainable spawning biomass [37]. Although the dolphinfish is not a small pelagic it has a similar life history as small pelagic fish.

2.3 Population dynamics models

Generalized depletion models estimate abundance at the start of the time series in the N_0 parameter. Abundance then drops and is reset to a higher value with every input of abundance due to recruitment, one for each year in the time series. Therefore, for each year, total initial abundance (i.e. in January of each year) can be obtained by rolling back recruitment pulses from the month of recruitment and adding that to abundance in December of the previous year. Rolling back entails using the natural mortality rate estimate M with reversed sign. Knowing also the mean weight per month (Fig. 5), monthly abundance can be transformed into biomass, B_t . The function `CatDynBSD` in `CatDyn` does this calculation using the delta method to propagate statistical uncertainty in N_0 , M , and mean weight, to B_t .

The estimated biomass time series extends at monthly time steps over the complete time series, but selected stock's biomass at a particular month to fit a surplus production model. This month was the month at which the mean coefficient of variation (CV) of the biomass estimate was the lowest, i.e. the month of the typically highest statistical precision. The main purpose of using a particular month of biomass estimate from each year is to have an annual time step in the surplus production model. Having an annual time step is convenient because it is possible to use the landings from years prior to 2015 as additional data to fit the surplus production model. Selecting the month with the least average (across years) CV of the biomass estimate helps have more precise estimates of parameters in the surplus production model.

The South-East Pacific region is affected by the periodic occurrence of the El Niño

Southern Oscillations (ENSO) leading to multi-annual periods of increased water temperature followed by multi-annual periods of colder or normal temperature [38]. These environmental oscillations may well affect the stock's population dynamics. We used NOAA's ENSO index [22] to define four environmental phases during our study period (Fig. 7). Then we defined eight hypotheses of biomass dynamics during the study period (Fig. 3). The first hypothesis was the null hypothesis that the biomass dynamics was a conventional Pella-Tomlinson dynamics with constant parameters during the whole study period, i.e.:

$$B_y = B_{y-1} + rB_{y-1} \left(1 - \left(\frac{B_{y-1}}{K} \right)^{p-1} \right) - C_{y-1}, p > 1, y_1 \leq y \leq y_{end} \quad (4)$$

where

- r is the intrinsic population growth rate,
- p is the symmetry of the production function,
- K is the carrying capacity of the environment,
- B_y is the biomass estimated from generalized depletion models, and
- C_{y-1} is the total annual catch during the previous fishing season.

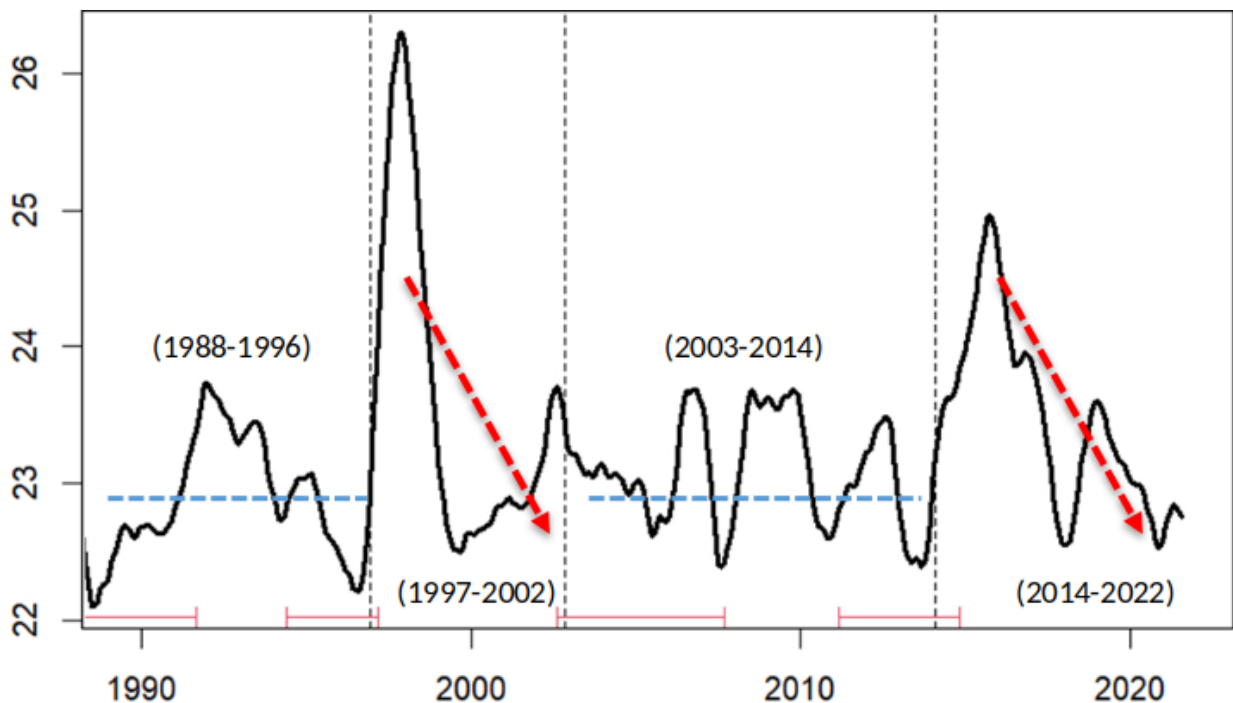


Figure 7: NOAA's ENSO index and the four environmental phases identified during the study period.

The seven alternative hypotheses were that the biomass dynamics, i.e. the Pella-Tomlinson model, had time-varying parameters that followed the environmental cycle. Thus the first alternative hypothesis had carrying capacity K varying from K_1 to K_2 to K_1 to K_2 during the environmental phases of cold, warm, cold and warm periods in Fig. 7. The second alternative hypothesis had the symmetry of the production function p varying from p_1 to p_2 to p_1 to p_2 during the four phases of the environmental cycle. The third hypothesis had the intrinsic population growth rate k varying from r_1 to r_2 to r_1 to r_2 during the four phases of the environmental cycle. The subsequent four hypotheses had pairs of parameter varying with the environmental cycle or all three parameters varying with the environmental cycle. In addition, we fitted each of these seven hypotheses in two variants, having initial biomass (in 2003) as a separate, fourth parameter in Pella-Tomlinson model or having it equal to the carrying capacity K . We selected the best working model by recourse to the Akaike Information Criterion (AIC) and further consideration of optimization quality criteria such as having all gradients close to zero and well-defined Hessian matrices.

The annual biomass and its standard deviation from fitting generalized depletion models and the annual biomass predicted by fourteen variants of the Pella-Tomlinson model are linked through a hybrid (marginal-estimated) likelihood function,

$$\ell_{HL}(\boldsymbol{\theta}_{PT}|\{\hat{B}_y\}) \propto -\frac{1}{2} \sum_{y_1}^{y_{end}} \left(\log(2\pi S_{\hat{B}_y}^2) + \frac{(\hat{B}_y - B_y)^2}{S_{\hat{B}_y}^2} \right) \quad (5)$$

where

- $\boldsymbol{\theta} = \{B_{y0}, K, r, p\}$ is the vector of parameters of the Pella-Tomlinson model in Eq. 4 plus one additional parameter for biomass in the year prior to the first year in the time series, 2003,
- $S_{\hat{B}_y}^2$ are the distinct numerical estimates of standard deviations of each annual biomass estimate from the fitted generalized depletion model (replacing the unknown distinct true standard deviations),
- \hat{B}_y are the maximum likelihood estimates of annual biomass from the fitted generalized depletion model, and
- B_y are the true annual biomass according to Eq. 4

From the fit of Pella-Tomlinson model, several biological reference points were calculated depending on the prevailing dynamics of the stock. The reference points were the MSY,

$$MSY = rK(p-1)p^{-p/(p-1)} \quad (6)$$

the biomass at the MSY,

$$B_{MSY} = Kp^{1/(1-p)} \quad (7)$$

and the latent productivity,

$$\dot{P} = \gamma MSY \frac{B_y}{K} \left(1 - \left(\frac{B_y}{K} \right)^{p-1} \right), \gamma = \frac{p^{p/(p-1)}}{p-1} \quad (8)$$

For each biological reference points, standard errors were computed using the delta method.

With reference to the latent productivity [39], this is a biological reference point analogous to MSY, but while MSY is a constant, the latent productivity varies with the biomass of the stock (compare Eq. 5 to Eq. 7). Thus the latent productivity is more relevant for stocks that tend to fluctuate because of environmental forces or because of their intrinsic population dynamics. For instance, in Roa-Ureta et al. [14] we found that the stock under study was fluctuating because of a high value of the intrinsic population growth rate, r . Thus MSY was not applicable and it was actually an excessive harvest rate. In the present case, if the stock was found to have a stationary equilibrium, MSY and B_{MSY} were computed as biological reference points, while if the stock was found to be fluctuating, the latent productivity was computed as the biological reference point. Both MSY and latent productivity can be used directly as sustainable harvest rates.

The analysis at this stage was programmed in ADMB [40] using ADMB-IDE 10.1 64 bits [41]. We created ADMB code for each of the eight environmental influence hypotheses and starting annual biomass leading to sixteen ADMB programs. Taking advantage of facilities of the ADMB system, parameter estimation was carried out by bounded or unbounded optimization, depending on the parameter and the model variant.

3 Results

3.1 Generalized depletion models

A total of 36 generalized model variants were fitted using CatDyn across the 192 months of effort and catch data by the four fleets, half of them using the *spg* and half the *CG* numerical methods for optimization. Initially, a set of 32 variants were fit with a specific assumption regarding the timing of the 64 recruitment events. Only two of those variants yielded a natural mortality rate higher than 0.1 per month and all variants predicted unrealistically high biomass. Three variants, characterized by the following specifications:

- variant 25: CG optimization algorithm, adjusted profile normal for the Peruvian artisanal fleet and the Peruvian fibreglass fleet, adjusted profile lognormal for the Ecuadorian artisanal fleet and the Ecuadorian fibreglass fleet,
- variant 29: CG optimization algorithm, adjusted profile normal for the Peruvian artisanal fleet, the Peruvian fibreglass fleet, the Ecuadorian artisanal fleet, and adjusted profile lognormal for the Ecuadorian fibreglass fleet,
- variant 31: CG optimization algorithm, adjusted profile normal for the catch data off all fleets,

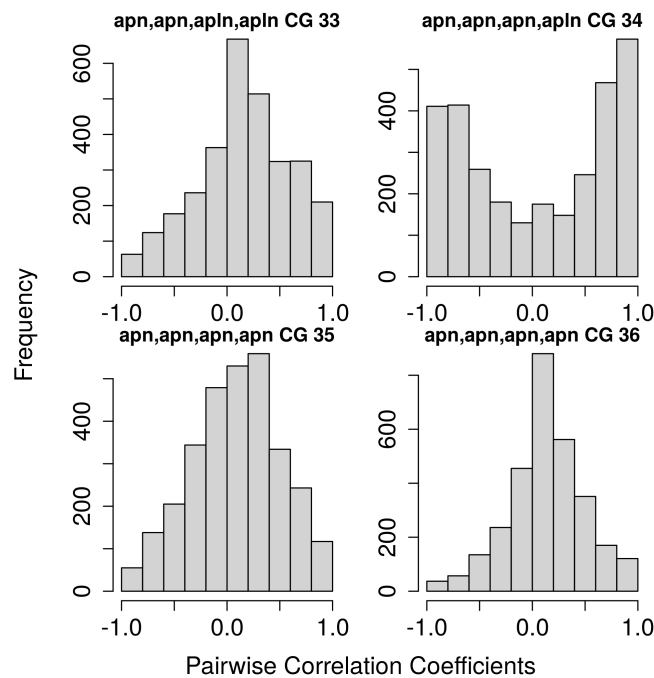


Figure 8: Correlation structure of estimates of the short list of four best variants of generalized depletion models fitted to catch data of the four fleets. The title of each histogram indicates the likelihood model (apn is adjusted profile normal and apln is adjusted profile lognormal for each fleet, numerical algorithm used for optimization, and model variant number

yielded the lowest biomass estimates and one of them also yielded a higher natural mortality estimate. These three variants were re-fitted using different starting values for recruitment parameters leading to variants 33, 34 and 35. These three additional variants yielded realistic biomass predictions and realistic natural mortality rate estimates. Variant 35 yielded the best correlation structure (Fig. 8) and lowest standard error of estimates. Small adjustments to the timing of some recruitment events in variant 35 led to fitting variant 36.

The AIC, useful to compare variants 35 and 36 because they were fit with the same likelihood model, was not conclusive. Nevertheless, variant 36 had only two gradients (for β of the Peruvian artisanal fleet and k of the Ecuadorian fibreglass fleet) larger than 1, less than all other 35 variants. Furthermore, had the best correlation structure (Fig. 8), reasonable natural mortality rate estimate and biomass predictions, and high statistical precision of the estimates for natural mortality rate and initial abundance, N_0 . Thus variant 36 was selected as the best generalized depletion model to fit the catch data of the four fleets.

The fit of variant 36 to the data from the four fleets is shown in Figs. 9-12. It can be seen in Fig. 9 that the selected model closely follows the catch data from the Peruvian artisanal fleet. Diagnostics plots at the bottom panels show good consistency with the model's assumptions, with a symmetric histogram of residuals, a shapeless cloud of residuals, and a diagonal quantile-quantile plot. "Biomass" is predicted biomass in the last month, December 2019, and "Catch" is the total catch by the four fleets in the last year, 2019.

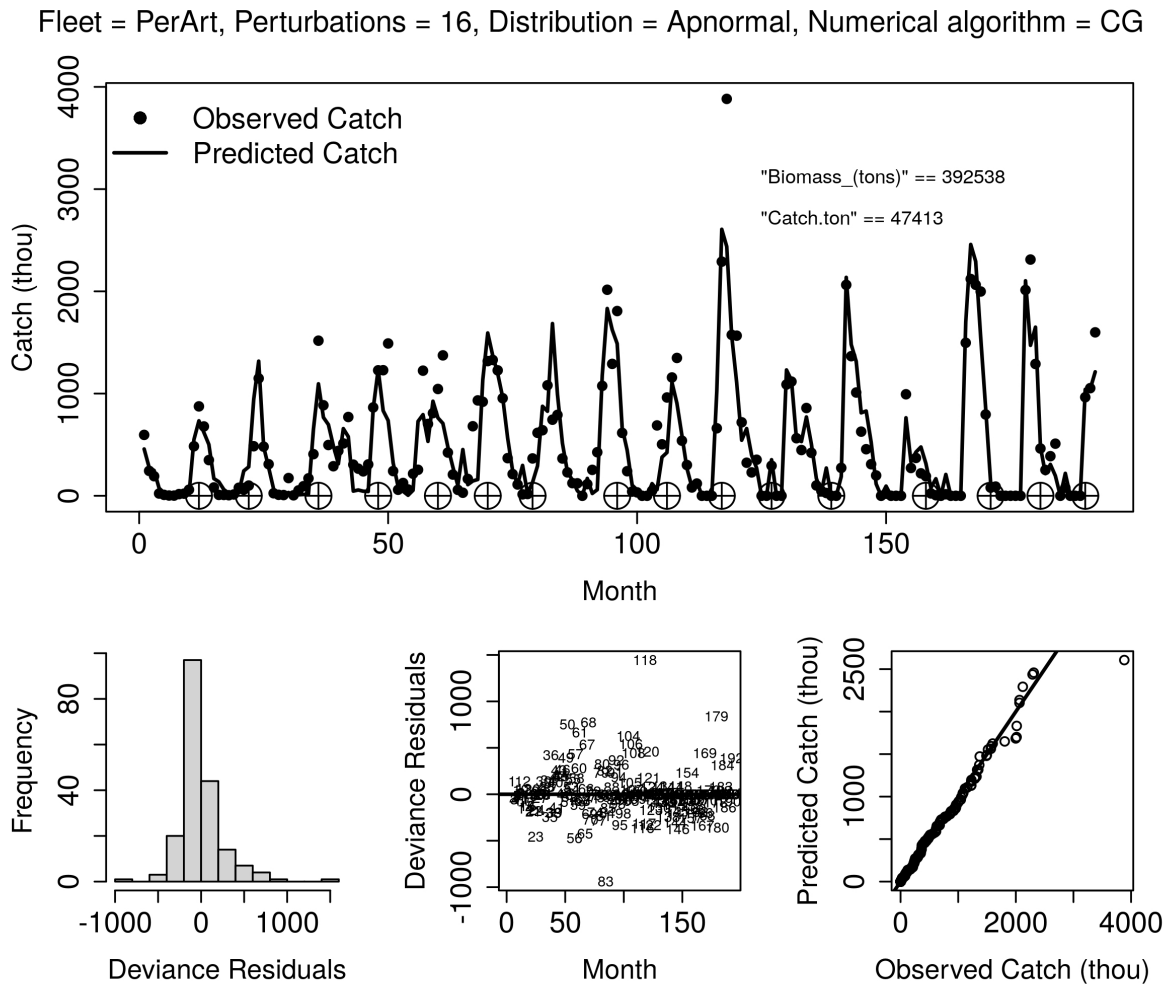


Figure 9: Top panel: Fit of the generalized depletion model to the Peruvian artisanal fleet catch data (top panel), with target symbols indicating the timing of annual recruitment. The catch is the total catch by all fleets in the last year, and the biomass is the biomass at the last month of the times series (December 2019). Bottom panels: from left to right, histogram of deviance residuals, deviance residual cloud, and quantile-quantile plot.

Table 1: Directly estimated parameters corresponding to the Peruvian artisanal fleet of the best generalized depletion model (variant 36) fitted the 192 months (2004 to 2019) of effort and catch data of the the dolphinfish fishery in the South-East Pacific. Variant 36 was fitted with the adjusted profile normal distribution for all four fleets, the CG numerical algorithm, recruitment timings as suggested by the catch spike statistic with a few adjustments. MLE: maximum likelihood estimate. CV: coefficient of variation. CVs not shown correspond to optimization failures for second order properties at particular parameters.

Parameter	Timing	MLE	CV (%)
M (month ⁻¹)		0.3390	5.0
N_0 (thousand)		99,934	18.3
Recruitment 2004 (thousand)	2004-12	155,253	
Recruitment 2005 (thousand)	2005-10	206,925	
Recruitment 2006 (thousand)	2006-12	155,811	
Recruitment 2007 (thousand)	2007-12	31,642	
Recruitment 2008 (thousand)	2008-12	7,619	275.4
Recruitment 2009 (thousand)	2009-10	143,019	98.4
Recruitment 2010 (thousand)	2010-7	425,94	143.6
Recruitment 2011 (thousand)	2011-12	1,484	316.6
Recruitment 2012 (thousand)	2012-10	88,123	50.6
Recruitment 2013 (thousand)	2013-9	298,651	14.6
Recruitment 2014 (thousand)	2014-7	579,369	14.0
Recruitment 2015 (thousand)	2015-7	3,319	279.0
Recruitment 2016 (thousand)	2017-2	586	228.6
Recruitment 2017 (thousand)	2018-3	5,879	200.4
Recruitment 2018 (thousand)	2019-1	666	317.5
Recruitment 2019 (thousand)	2019-10	321,265	
k (1/days)		0.00008558	
α		0.9443	
β		0.7060	

Fleet = PerFib, Perturbations = 16, Distribution = Apnormal, Numerical algorithm = CG

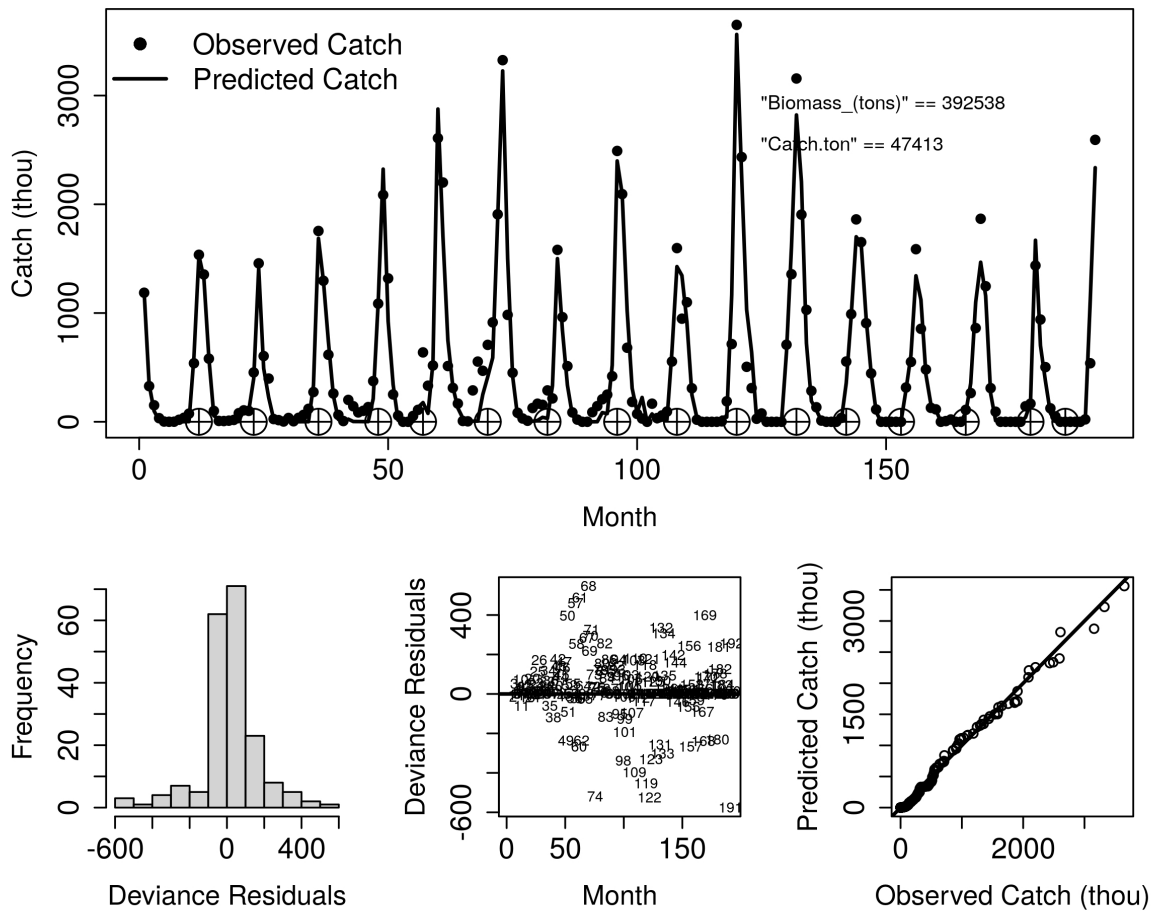


Figure 10: Top panel: Fit of the generalized depletion model to the Peruvian fibreglass fleet catch data (top panel), with target symbols indicating the timing of annual recruitment. The catch is the total catch by all fleets in the last year, and the biomass is the biomass at the last month of the times series (December 2019). Bottom panels: from left to right, histogram of deviance residuals, deviance residual cloud, and quantile-quantile plot.

Table 2: Directly estimated parameters corresponding to the Peruvian fibreglass fleet of best generalized depletion model fitted (variant 36) the 192 months (2004 to 2019) of effort and catch data of the the dolphinfish fishery in the South-East Pacific. MLE: maximum likelihood estimate. Variant 36 was fitted with the adjusted profile normal distribution for all four fleets, the CG numerical algorithm, recruitment timings as suggested by the catch spike statistic with a few adjustments. CV: coefficient of variation. CVs not shown correspond to optimization failures for second order properties at particular parameters.

Parameter	Timing	MLE	CV (%)
M (month ⁻¹)		0.3390	5.0
N_0 (thousand)		99,934	18.3
Recruitment 2004 (thousand)	2004-12	13,205	
Recruitment 2005 (thousand)	2005-11	20,169	
Recruitment 2006 (thousand)	2006-12	13,121	
Recruitment 2007 (thousand)	2007-12	66,906	
Recruitment 2008 (thousand)	2008-9	223,212	21.2
Recruitment 2009 (thousand)	2009-10	8,744	1118.5
Recruitment 2010 (thousand)	2010-10	48,159	65.6
Recruitment 2011 (thousand)	2011-12	1,292	340.6
Recruitment 2012 (thousand)	2012-12	68,577	
Recruitment 2013 (thousand)	2013-12	740	246.1
Recruitment 2014 (thousand)	2014-12	23,045	92.5
Recruitment 2015 (thousand)	2015-10	119,023	21.1
Recruitment 2016 (thousand)	2016-9	107,607	24.1
Recruitment 2017 (thousand)	2017-10	215,594	14.8
Recruitment 2018 (thousand)	2018-11	127,903	18.1
Recruitment 2019 (thousand)	2019-7	3,421	384.8
k (1/days)		0.0000003386	
α		1.0901	2.3
β		1.2360	0.1

Fleet = EcuArt, Perturbations = 16, Distribution = Apnormal, Numerical algorithm = CG

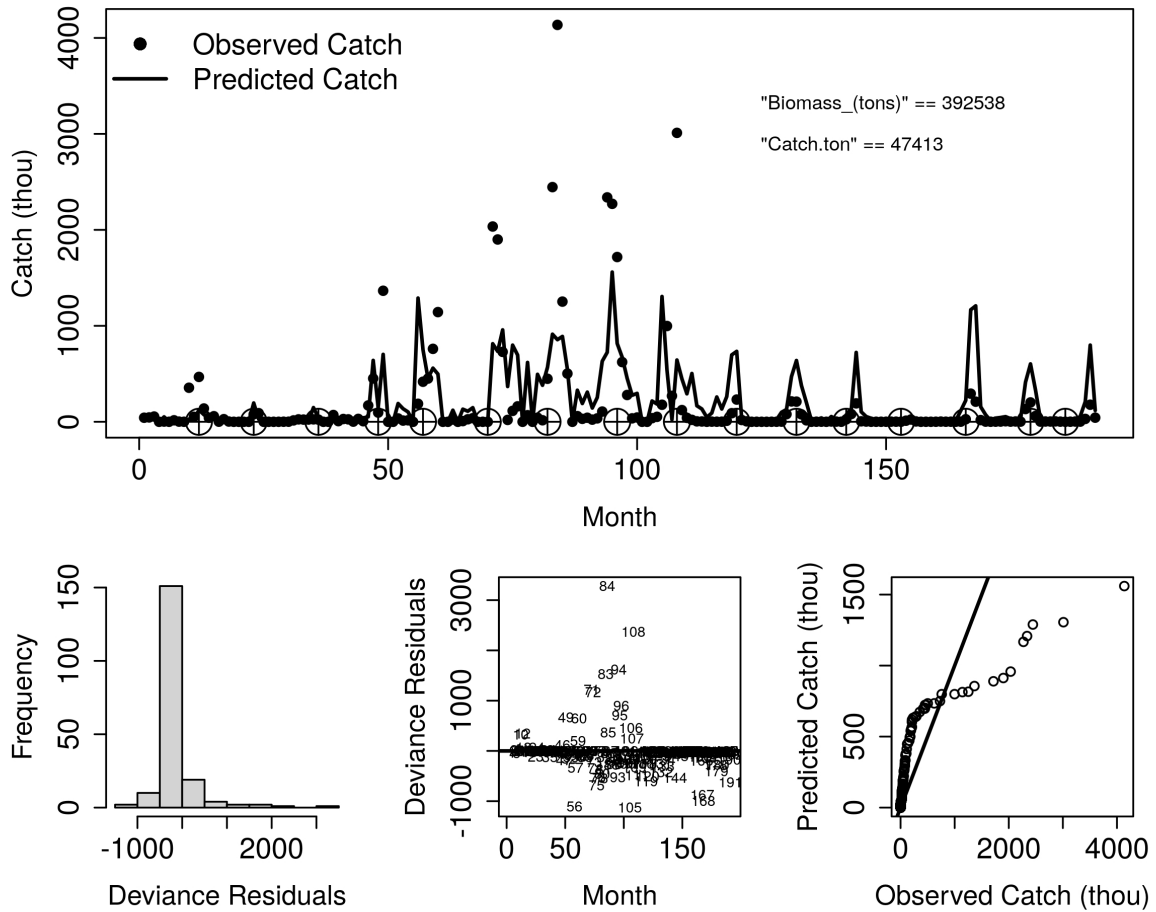


Figure 11: Top panel: Fit of the generalized depletion model to the Ecuadorian artisanal fleet catch data (top panel), with target symbols indicating the timing of annual recruitment. The catch is the total catch by all fleets in the last year, and the biomass is the biomass at the last month of the times series (December 2019). Bottom panels: from left to right, histogram of deviance residuals, deviance residual cloud, and quantile-quantile plot.

Table 3: Directly estimated parameters corresponding to the Ecuadorian artisanal fleet of best generalized depletion model fitted (variant 36) the 192 months (2004 to 2019) of effort and catch data of the the dolphinfish fishery in the South-East Pacific. MLE: maximum likelihood estimate. Variant 36 was fitted with the adjusted profile normal distribution for all four fleets, the CG numerical algorithm, recruitment timings as suggested by the catch spike statistic with a few adjustments. CV: coefficient of variation. CVs not shown correspond to optimization failures for second order properties at particular parameters.

Parameter	Timing	MLE	CV (%)
M (month ⁻¹)		0.3390	5.0
N_0 (thousand)		99,934	18.3
Recruitment 2004 (thousand)	2004-11	7,646	
Recruitment 2005 (thousand)	2005-12	4,384	
Recruitment 2006 (thousand)	2006-12	7,734	
Recruitment 2007 (thousand)	2007-12	25,468	58.0
Recruitment 2008 (thousand)	2009-1	4,620	1540.8
Recruitment 2009 (thousand)	2009-10	24,218	
Recruitment 2010 (thousand)	2010-12	149,946	20.5
Recruitment 2011 (thousand)	2011-10	6,993	
Recruitment 2012 (thousand)	2012-12	43,867	23.8
Recruitment 2013 (thousand)	2014-1	3,693	
Recruitment 2014 (thousand)	2015-3	30,006	24.8
Recruitment 2015 (thousand)	2016-1	1,233	384.3
Recruitment 2016 (thousand)	2016-12	1,226	2460.6
Recruitment 2017 (thousand)	2017-7	476	377.7
Recruitment 2018 (thousand)	2019-1	1,184	679.6
Recruitment 2019 (thousand)	2019-7	1,487	
k (1/days)		0.0001268	
α		2.0424	4.3
β		0.5236	14.4

Fleet = EcuFib, Perturbations = 16, Distribution = Apnormal, Numerical algorithm = CG

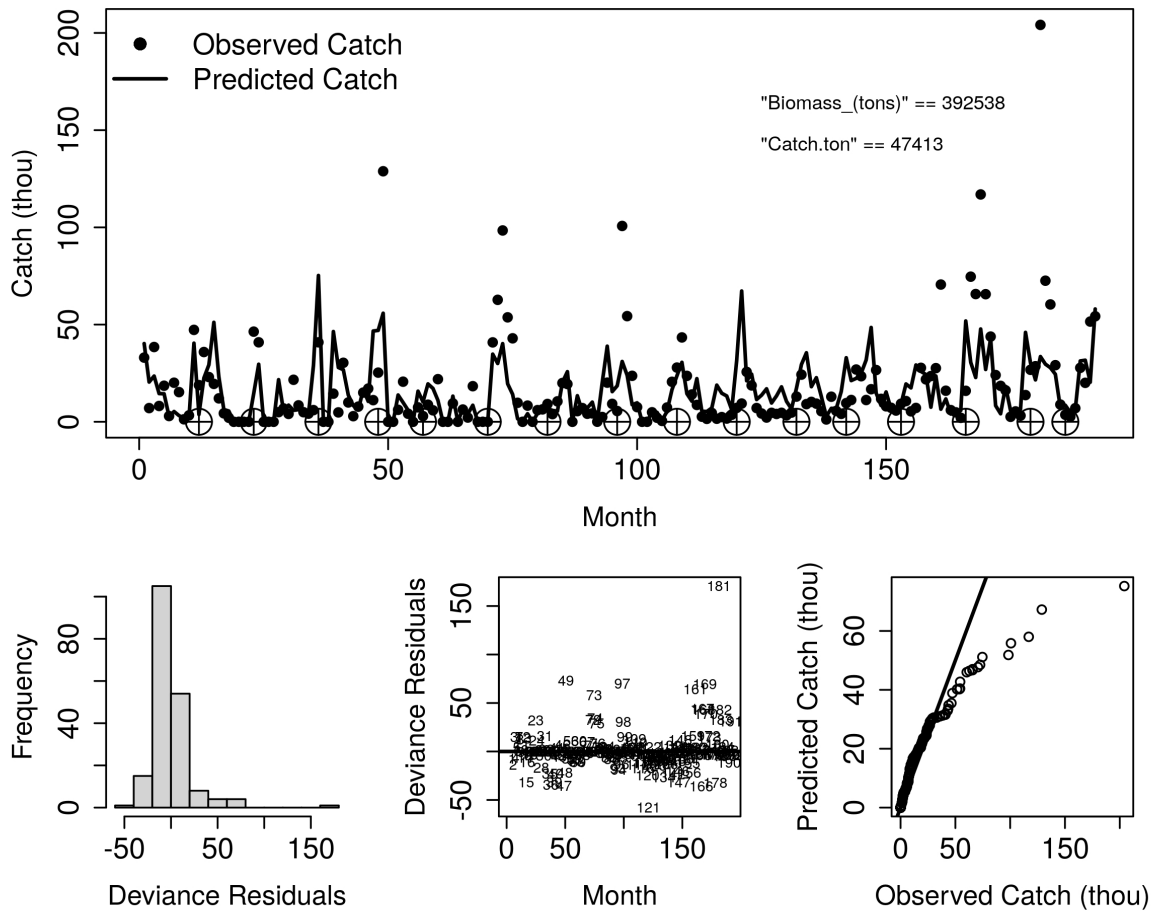


Figure 12: Top panel: Fit of the generalized depletion model to the Ecuadorian fibreglass fleet catch data (top panel), with target symbols indicating the timing of annual recruitment. The catch is the total catch by all fleets in the last year, and the biomass is the biomass at the last month of the times series (December 2019). Bottom panels: from left to right, histogram of deviance residuals, deviance residual cloud, and quantile-quantile plot.

Table 4: Directly estimated parameters corresponding to the Ecuadorian fibreglass fleet of best generalized depletion model fitted (variant 36) the 192 months (2004 to 2019) of effort and catch data of the the dolphinfish fishery in the South-East Pacific. Variant 36 was fitted with the adjusted profile normal distribution for all four fleets, the CG numerical algorithm, recruitment timings as suggested by the catch spike statistic with a few adjustments. MLE: maximum likelihood estimate. CV: coefficient of variation. CVs not shown correspond to optimization failures for second order properties at particular parameters.

Parameter	Timing	MLE	CV (%)
M (month ⁻¹)		0.3390	5.0
N_0 (thousand)		99,934	18.3
Recruitment 2004 (thousand)	2004-12	7,646	
Recruitment 2005 (thousand)	2005-12	16,980	
Recruitment 2006 (thousand)	2007-1	68,377	48.0
Recruitment 2007 (thousand)	2008-1	2,696	536.1
Recruitment 2008 (thousand)	2008-12	88,454	48.5
Recruitment 2009 (thousand)	2009-11	44,985	
Recruitment 2010 (thousand)	2010-12	36,395	28.0
Recruitment 2011 (thousand)	2012-1	6,424	
Recruitment 2012 (thousand)	2013-1	693	254.4
Recruitment 2013 (thousand)	2013-12	2,655	
Recruitment 2014 (thousand)	2014-11	2,232	365.5
Recruitment 2015 (thousand)	2015-12	35,557	25.6
Recruitment 2016 (thousand)	2017-1	5,575	
Recruitment 2017 (thousand)	2017-12	503	367.0
Recruitment 2018 (thousand)	2019-1	2,101	
Recruitment 2019 (thousand)	2019-11	2,779	
k (1/days)		0.001884	176.3
α		0.9377	14.8
β		0.3131	37.4

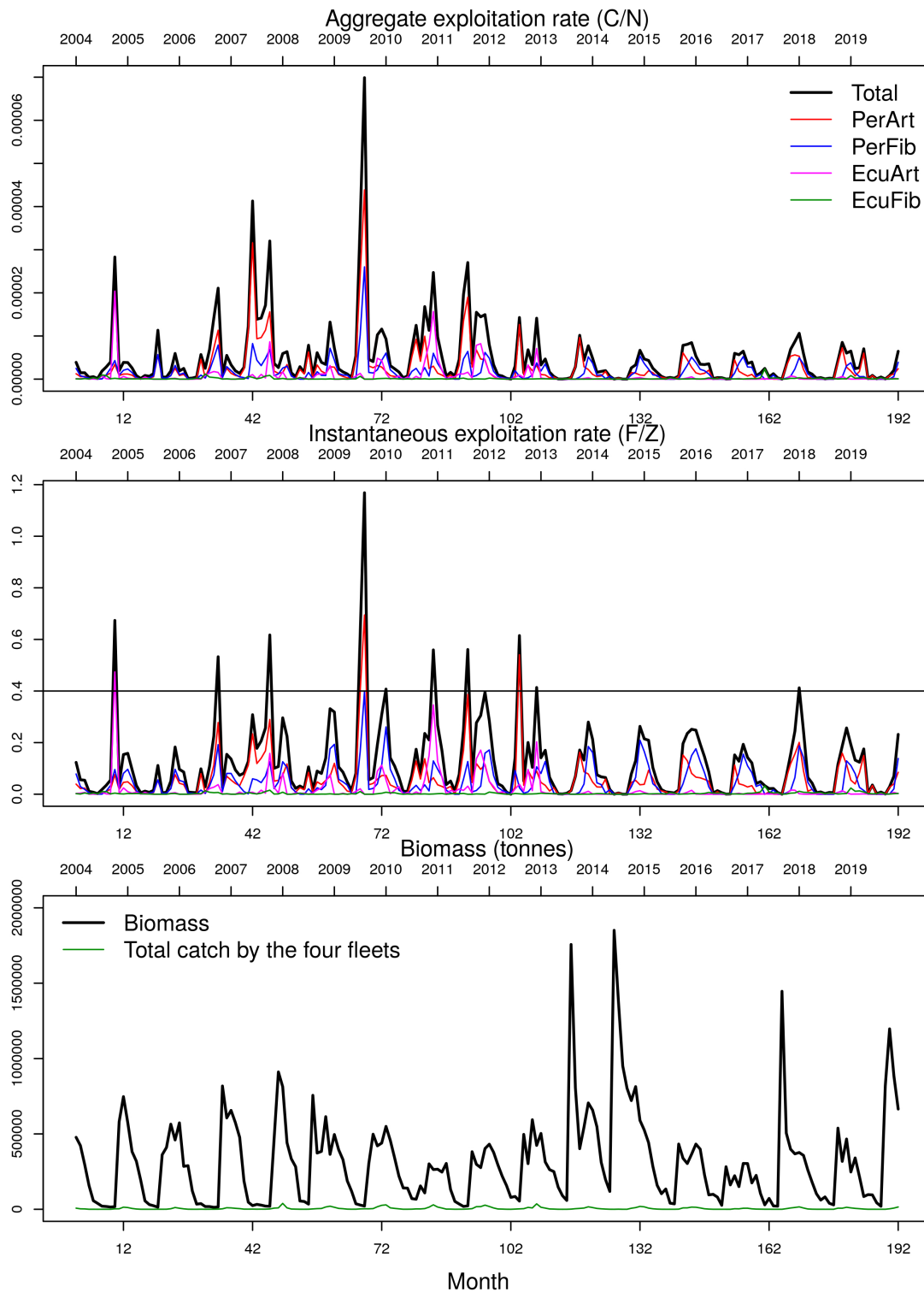


Figure 13: Top panel: Aggregate exploitation rate for each fleet and in total. Middle panel: instantaneous exploitation rate per fleet and in total. Bottom panel: stock biomass and catch in weight.

The model indicates that the catch taken during the last year of the time series was only 12% of the biomass left available at the end of the year, which is a very moderate exploitation rate. The fit of the model to the data from the Peruvian fibreglass fleet is even better (Fig. 10), with excellent agreement between model and data (top panel), symmetrical residual histogram, shapeless residual cloud, and excellent quantile-quantile plot. However, the fit of the model to the Ecuadorian artisanal fleet (Fig. 11) is much poorer, with numerous high catches that are not well followed by the model (top panel), skewed residual histogram, and far from diagonal quantile-quantile plot. The fit of the model to the Ecuadorian fibreglass fleet (Fig. 12) is somewhat better though still poor, with numerous high catches not well predicted by the model (top panel), slightly skewed residual histogram (month 181 is a highly positive residual), nearly shapeless residual cloud (except for month 181), and nearly all lower quantiles following on the diagonal.

Parameter estimates from the selected generalized depletion model are presented in Tables 1-4. Monthly natural mortality M is very high, as expected considering the short life history of the dolphinfish [11]. Initial abundance N_0 was in the order of a hundred million. Recruitment estimates to the Peruvian artisanal fleet (Table 1) vary from a few million to several hundred million. Catches are nearly proportional to effort and hyper-stable to abundance. Recruitment estimates to the Peruvian fibreglass fleet (Table 2) vary from a few hundred thousand to a few hundred million. Catches are nearly proportional to both effort and abundance. Recruitment estimates to the Ecuadorian artisanal fleet (Table 3) vary from a few hundred thousand to a few tens of million. Catches are synergistic to effort and hyper-stable to abundance. Recruitment estimates to the Ecuadorian artisanal fleet (Table 3) vary from a few hundred thousand to a few tens of million. Catches are proportional to effort and hyper-stable to abundance. Many standard errors (and thus CVs) could not be calculated signifying problems with the curvature of the likelihood function close to the maximum.

The aggregate exploitation rate is very low, reaching a maximum of 0.006% fish caught with respect to total abundance happening over the sixth year of the time series, while usually at every month total catch takes 0.0002% of all available fish (Fig. 13, top panel). The instantaneous exploitation rate (Fig. 13, middle panel) remains most of the months under 40%, the reference point obtained by Patterson [37], crossing that threshold just a few times and for one-month periods. The biomass and catch time series shows that at specific months in each year total catch in biomass approaches stock biomass while most of the months the latter is much higher than the former.

3.2 Population dynamics models

Estimation of the biomass monthly time series and the standard error of biomass estimates using the function `CatDynBSD` in the extended `CatDyn` software yielded estimates that on average, were most precise in the month of November, with an average CV of 225%, which is very imprecise although less imprecise than in other months. Thus, the biomass estimate in November was selected to fit Pella-Tomlinson surplus production model under eight hypotheses of environmental influence.

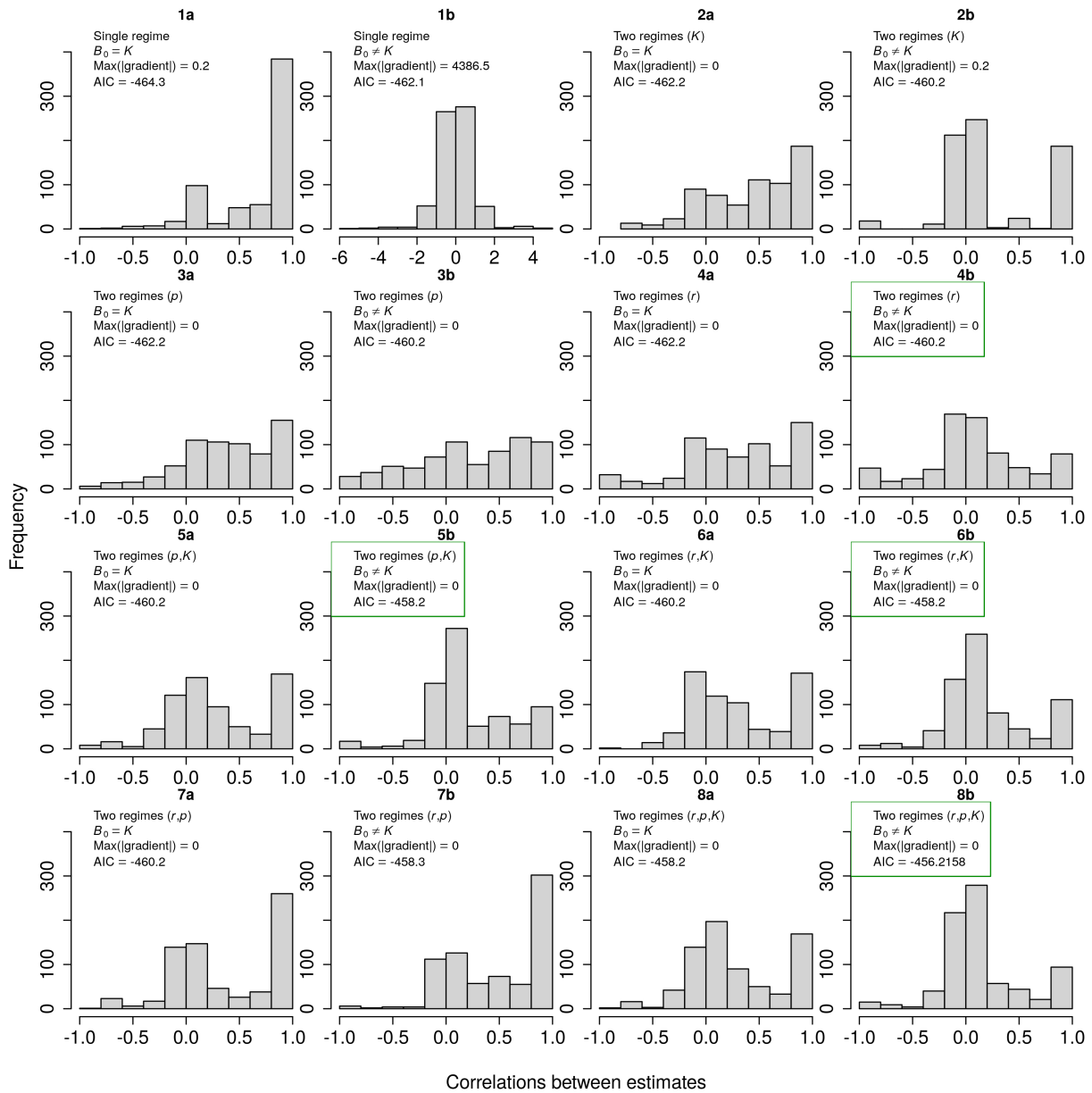


Figure 14: Pairwise correlations between parameter estimates (including 3 or four parameters in Pella-Tomlinson and 33 annual biomass predictions) and model selection criteria of sixteen hypotheses for the biomass population dynamics of the dolphinfish stock in the South-Eastern Pacific. Single regime (top left panels) are null hypothesis models with no influence of environmental cycles. Two regimes are hypotheses that involve changes in K, p or r singly, or in pairs or the trio of parameters of Pella-Tomlinson surplus production model. Panels with a green border are the best working models.

Fig. 14 shows the pairwise correlations among parameter estimates of Pella-Tomlinson surplus production model under sixteen hypotheses of environmental influence. Histograms of correlation coefficients that are centered around zero are produced by models with param-

eter that are adequately identifiable (i.e. each parameter play a useful role). Furthermore, model variants with the lowest AIC and largest gradient in absolute value close to zero are best working models. There are four of these models, marked with a green border in Fig. 14, and among those four best working models, the variant labelled as 4b in Fig. 14 had the lowest AIC and the smallest standard errors of parameter estimates. This variant corresponded to the hypothesis that the biomass dynamics of the dolphinfish was influenced by environmental cycles through changes in the intrinsic rate of growth r .

The fitted Pella-Tomlinson dynamics from the best Pella-Tomlinson model (variant 4b in Fig. 14) as well as biomass estimates from the best generalized depletion model and the time series of total annual catch, are shown in Fig. 15. Biomass estimates from CatDyn running in R and the Pella-Tomlinson surplus production biomass running in ADMB show good agreement. The Pella-Tomlinson model shows that the stock has a tendency to undergo marked fluctuations and that the most recent status of the stock is the most uncertain part of the time series. The stock biomass has been well above landings for a long period that ended in 2016, when there was a sharp drop in biomass. This observed decline in biomass was followed by an equally fast recovery in stock biomass over the next 2 years. Overall, stock biomass shows fluctuation about a constant mean close to 350 thousand tonnes.

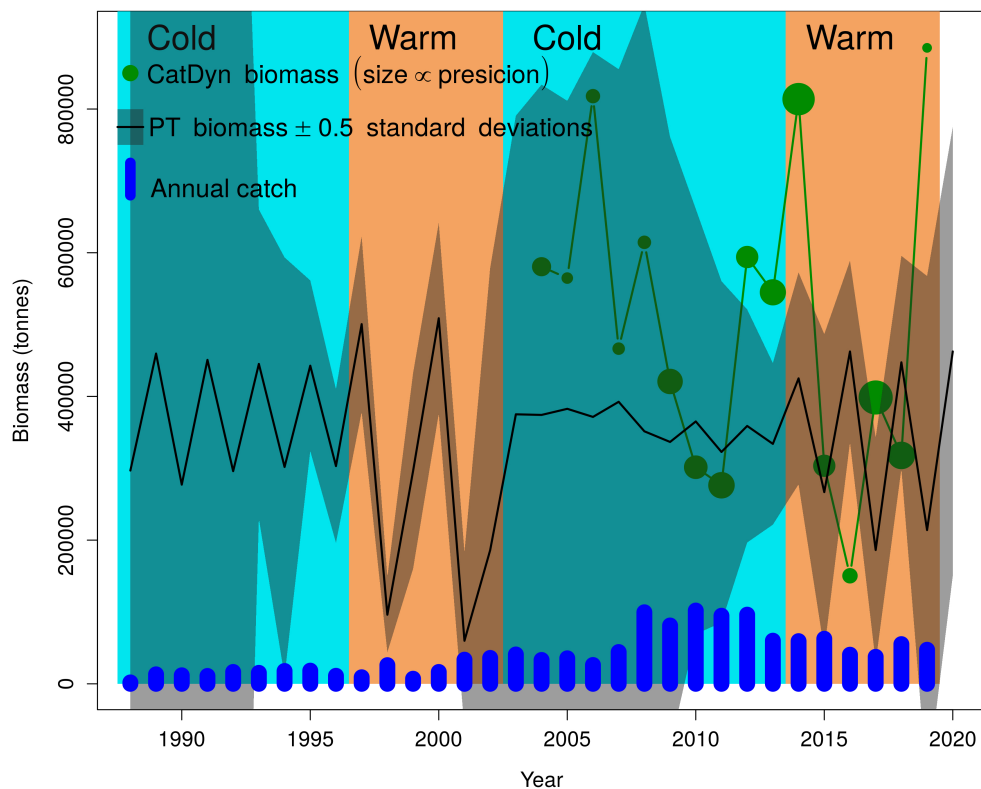


Figure 15: November stock biomass estimated by the best generalized depletion model in the extended CatDyn software (variant 36), best Pella-Tomlinson model of population dynamics (variant 4b), and total annual catch by four fleets operating in the dolphinfish fishery in the South-Eastern Pacific.

Parameters of the Pella-Tomlinson model were fitted with good precision (Table 5), both those directly estimated by optimization and the derived parameters MSY , B_{MSY} and $B_{\dot{P}}$. The exception is the average total latent productivity (average latent productivity + landings) which is estimated with poor precision. The MSY estimate is very high, actually six times higher than the average catch of the four fleets over the time series. Conversely, the total average latent productivity a little double the average catch of the four fleets over the time series. This is because the stock has a fluctuating dynamics and therefore the MSY is not applicable. The total average latent productivity is the sustainable harvest rate for fluctuating stocks. Both the estimated intrinsic rate of population growth r and the symmetry of the production function p are high, making the stock highly productive.

Table 5: Directly estimated parameters from the best Pella-Tomlinson model (B_0 , K , r_1 , r_2 , p) and derived biological reference points (MSY_1 , MSY_2 , B_{MSY} , \dot{P}_1 , \dot{P}_2) for the dolphinfish in the South-East Pacific according to parameterization in Eqs. 4, 6-8, likelihood model in Eq. 5. \dot{P}_1 and \dot{P}_2 are the annually averaged total latent productivity under the cold and warm environmental regimes, respectively (see Eq. 5). Mean catches during cold and warm periods are calculated within the 2004 to 2019 interval of years. B_{MSY} does not change from the cold to the warm periods of the environmental cycle because B_{MSY} does not depend on r (see Eq. 7).

Regime	Parameter	Estimate	Standard error	CV (%)
Period 1	B_0 (tonnes)	296,880	94,576,000	31857.0
Cold, r_1	K (tonnes)	393,970	176,420	44.8
$r_1 \rightarrow r_2$	r_1 (yr ⁻¹) (Cold)	2.450	4.444	181.4
Period 2	r_2 (yr ⁻¹) (Warm)	3.235	5.835	180.4
Warm, r_2	p	1.913	1.566	81.9
$r_2 \rightarrow r_1$	MSY_1 (tonnes) (Cold)	225,481	155,486	69.0
Period 3	MSY_2 (tonnes) (Warm)	299,203	185,832	62.1
Cold, r_1	B_{MSY} (tonnes)	193,356	99,986	51.7
$r_1 \rightarrow r_2$	\dot{P}_1 (tonnes) (Cold)	91,386		
Period 4	Mean catch (tonnes) (Cold)	41,569		
Warm, r_2	\dot{P}_2 (tonnes) (Warm)	70,731		
(Variant 4b)	Mean catch (tonnes) (Warm)	35,969		

4 Discussion

This study shows that the stock of the dolphinfish in the South-East Pacific was being harvested in sustainable fashion up to the last year of the available time series of data (2019). In fact, average landings by the four fleets over the 2004 to 2019 period are close to half of the sustainable harvest rate in each of two periods in the environmentally-driven cycle of population dynamics. These harvest rates have been estimated at close to 91 thousand tonnes during the cold period and close to 71 thousand tonnes during the warm period. Average catches between 2004 and 2019 have been around 42 and 36 thousand tonnes in

the cold and warm periods, respectively, tracking well the differences in sustainable harvest rates estimated here.

Aires-da-Silva *et al.* [21] have described the combined Peruvian-Ecuadorian fishery as a data poor fisheries and have characterized the stock dynamics as highly productive, variable and fast. Our results confirm that description by showing that the stock has a high intrinsic rate of population growth (r) making it a resilient stock, that may recover quickly from low biomass, high mortality rate and fast biomass production function. In addition, the stock has a maximum of the production function close to symmetry, though slightly skewed towards lower biomass. Parameter are estimated with reasonable precision with the exception of initial biomass and the r s.

In their assessment of the same stock Aires-da-Silva *et al.* [21] concluded that the stock was being harvested at close to MSY levels. Our results here support the overall conclusion that the stock is not overfished and not experiencing overfishing but they also indicate that the current harvest is well below maximum sustainable harvest rates while Aires-da-Silva *et al.* found that the harvest rate was close to MSY. The difference in results may arise from a number of issues acting in conjunction or separately. First, we used different data. Our database was more extended (from January 2004 to December 2019) than the database compiled by Aires-da-Silva *et al.* (July 2007 to June 2015). In addition, for the period covered by Aires-da-Silva *et al.* we have higher catches from Ecuadorian fleets between 2008 and 2012. Second, the stock assessment by Aires-da-Silva *et al.* is based on length frequency data and CPUE indices of relative abundance while our assessment is based on the effort-catch dynamics (generalized depletion models) and the aggregate biomass dynamics (Pella-Tomlinson surplus production model). Aires-da-Silva *et al.* length-structured model is more complex from the population dynamics point of view and it has to make several assumptions to simplify the problem. Authors list 8 such assumptions but principal among these are three:

- Fixed natural mortality rate ($M = 1 \text{ yr}^{-1}$ for both sexes);
- Fixed Steepness (h) of the stock-recruitment relationship ($h = 1$); and
- The CPUE time series of the Ecuadorian artisanal fishery was chosen as the most reliable index of abundance to calibrate the stock assessment model. For this reason, its coefficient of variation (CV) was fixed at 0.2.

In this work we have estimated the natural mortality rate from the data, inside the stock assessment model, by maximum likelihood and this objective estimate turned out to be much higher than the value assumed by Aires-da-Silva *et al.*. Fixing natural mortality too low in a stock assessment would lead to under-estimation of fish abundance because less fish are needed to explain catches. This alone could explain why Aires-da-Silva *et al.* obtained less dolphinfish abundance than in our assessment. Fixing the steepness at a very high value, as done by Aires-da-Silva *et al.*, would ameliorate somewhat the under-estimation of abundance due to a low fixed value for natural mortality but our results show that the natural mortality rate is over 3 times higher than the value assumed by Aires-da-Silva *et al.* so any amelioration caused by fixing the steepness very high may not be sufficient to compensate

for a too low natural mortality rate. Furthermore, the decision by Aires-da-Silva *et al.* to give more weight to the Ecuadorian CPUE index of abundance because it produced a best fit in their assessment, may have negative implications. In our analysis, we used a catch and effort database compiled by Ecuadorian experts that differed substantially from the time series used by Aires-da-Silva *et al.*, especially between 2008 and 2012. Thus their better fit to Ecuadorian CPUE would be an artifact of missing catch data. In addition, our results also show that the Ecuadorian data, from both fleets, is less well fit to depletion models because of more extreme (high) values of catch. This characteristic of the Ecuadorian data may have affected the assessment by Aires-da-Silva *et al.*. Third, we distinguished four fleets operating in the fishery, two in each country EEZ, while Aires-da-Silva *et al.* aggregated all national fleets and added a third fleet (tuna purse seiners) yielding bycatch of dolphinfish. National fleets in Ecuador and Perú are divided into two groups, artisanal and coastal. The artisanal fleets of both countries conduct long fishing trips, extending over several days in oceanic waters, while fibreglass boats can only operate in coastal waters for short fishing trips. This aspect may affect the building of aggregate CPUE indices of abundance.

The stock assessment model developed and implemented in this work needs further work to calculate standard errors of average total latent productivity estimates. These estimates depend on a complex covariance structure between annual biomass estimates and parameters of the Pella-Tomlinson model. Further work utilizing the delta method or ADMB code is needed to complete these steps.

In the South-East Pacific, environmentally driven transitions in population dynamics, connected to well know cycles in oceanographic and atmospheric processes in the whole Equatorial Pacific, have a significant impact on sustainable harvest rates for fishers operating on the dolphinfish stock. Normal or cold periods have higher sustainable harvest rates than warm, ENSO periods, and fishers have corresponding lower catches when sustainable harvest rates are lower. This happens without knowledge of sustainable harvest rates in cold versus warm periods of the environmental cycle. This coincidence implies that there could be natural processes that force less fishing yield when productivity is lower in this fishery.

During warm, ENSO periods, the stock experiences wider fluctuations in abundance compared with cold, normal periods of the environmental cycle. Nevertheless, these periods of warmer waters and wider fluctuations provide a window of opportunity for better determination of the population dynamics by the stock assessment model. This is well represented by much narrower bands of statistical error around the estimated biomass trajectory of the stock. The mathematical reason for wider fluctuations during warm water periods is that r is higher. Therefore the environmental cycle drives an intrinsic population cycle into wider or narrower fluctuations, thus providing direct evidence of the importance of ecosystem considerations when developing best management actions aiming at sustainable harvest rates.

5 Conclusions

1. A stock assessment database of monthly catch, effort and mean weight data for the dolphinfish in the South-East Pacific (Peru and Ecuador) with the activity of four

longline fleets, spanning 2004 to 2019, has been compiled from the data collection programs of IMARPE and IPIAP experts.

2. A statistical stock assessment methodology and its code in the R language of statistical programming and in ADMB, as well as binary storage of the database and programming objects, is now available for updated assessment of the dolphinfish in the South-East Pacific (Peru and Ecuador) as more data are collected.
3. The stock assessment methodology was applied to the dolphinfish in the South-East Pacific (Peru and Ecuador) data and the four fleets generating results with a generally acceptable level of statistical precision and biological realism.
4. Among a set of 36 variants of generalized depletion models, defined by 32 combinations of likelihood functions per fleet and numerical method of optimization, plus 4 adjustments to initial values and some months of recruitment, the best model was one with normal distributions for the data from all four fleets and CG numerical optimization algorithm.
5. Natural mortality rates are very high (0.339 per month) and estimated with good statistical precision (5% CV), annual recruitment pulses to the whole region and the four fleets vary from a few million to a few hundred million fish, and catches are generally proportional to fishing effort and hyper-stable to abundance.
6. Aggregate and instantaneous exploitation rates (as well as fishing mortality) were well within sustainable levels for the whole length of the time series 2004-2019.
7. Analysis of the NOAA indicator of ENSO determined the existence of an environmental cycle with four periods, starting with a cold, normal period (1988-1996), followed by a warm, ENSO period (1997-2002), followed by a cold period (2003-2014), and ending in a warm period (2014-2019).
8. The biomass dynamics of the stock in the region is driven by environmental cycles connected to the ENSO, leading to changes in the intrinsic rate of population growth.
9. During warm, ENSO years the stock has lower sustainable harvest rates and wider fluctuations than during normal, cold water periods.
10. Actual harvest rates during warm, ENSO years as well during cold, normal periods have been close to half the sustainable harvest rates of each period, further demonstrating that the stock was not over-fished up to 2019.

6 Management Advice

This management advice is exclusively connected to the biological condition of the stock of dolphinfish in the South-East Pacific and to key fishery factors such as fishing mortality and environmental fluctuations. Thus it is made without consideration of the wider social and economic context of the fishery.

1. Continue the data collection program and the growth of the stock assessment database to update the assessments at annual time steps.
2. Explore further improvements in the stock assessment database by extending introducing a local length-weight relationship.
3. Update the stock assessment with data from years after 2019 and update the status of the fishery.
4. Conditional upon confirmation with further data of the status of the stock, develop a plan to gradually increase fishing effort and thus yield better outcomes from the fishery for fishers, consumer and exporters, up to a level to be determined and below the level required to harvest the total average latent productivity annually.

List of Figures

1	Map of Peruvian and Ecuadorian EEZs where the fishery is conducted. . . .	2
2	World and country landings and contrast between catch data in the stock assessment database and in FAO databases [23] for the two countries.	3
3	Schematic representation of the stock assessment modelling approach. At Stage 1, catch (C), fishing effort (E) and mean weight in the catch (W) data at monthly time steps from Jan. 2004 to Dec. 2019 is used to fit a multi-annual four-fleets generalized depletion model. From the output of this model, annual biomass estimates (B, 2004 to 2019) and their standard errors (S) in addition to total annual catch (C, 1988 to 2019) are used in Stage 2 to fit a time-varying parameters Pella-Tomlinson model. Eight alternative hypotheses are tested: constant parameters (null hypothesis) and seven alternative hypotheses where parameters K , p and r vary singly or in pairs or trios from warm to cold water regimes.	4
4	Pattern of missing data in the original database compiled for stock assessment of the stock of dolphinfish in the South-Eastern Pacific (Peru and Ecuador). The left panel is a histogram of months with missing data per variable. The right panel is the number of months missing data at particular combinations of the variables. The variables are <i>WeightPer</i> : mean weight in Peruvian catches; <i>EffEcuFib</i> : total fishing effort in the Ecuadorian fibreglass fleet; <i>LengthEcu</i> : mean length in Ecuadorian catches; <i>CatEcuFib</i> : total catch in the Ecuadorian fibreglass fleet; <i>EffPerArt</i> : total fishing effort in the Peruvian artisanal fleet; <i>EffEcuArt</i> : total fishing effort in the Ecuadorian artisanal fleet; <i>CatEcuArt</i> : total catch in the Ecuadorian artisanal fleet; <i>CatPerArt</i> : total catch in the Peruvian artisanal fleet; <i>EffPerFib</i> : total fishing effort in the Peruvian fibreglass fleet; and <i>CatPerFib</i> : total catch in the Peruvian fibreglass fleet.	6
5	Effort and catch data in four fleets operating in the South-East Pacific (Peru and Ecuador). PerArt: Peruvian artisanal; PerFib: Peruvian fibreglass; EcuArt: Ecuadorian artisanal; EcuFib: Ecuadorian fibreglass.	7
6	Mean weight time series used to transform catch in weight to catch in numbers.	8
7	NOAA's ENSO index and the four environmental phases identified during the study period.	13
8	Correlation structure of estimates of the short list of four best variants of generalized depletion models fitted to catch data of the four fleets. The title of each histogram indicates the likelihood model (apn is adjusted profile normal and apln is adjusted profile lognormal for each fleet, numerical algorithm used for optimization, and model variant number	16
9	Top panel: Fit of the generalized depletion model to the Peruvian artisanal fleet catch data (top panel), with target symbols indicating the timing of annual recruitment. The catch is the total catch by all fleets in the last year, and the biomass is the biomass at the last month of the times series (December 2019). Bottom panels: from left to right, histogram of deviance residuals, deviance residual cloud, and quantile-quantile plot.	17

10	Top panel: Fit of the generalized depletion model to the Peruvian fibreglass fleet catch data (top panel), with target symbols indicating the timing of annual recruitment. The catch is the total catch by all fleets in the last year, and the biomass is the biomass at the last month of the times series (December 2019). Bottom panels: from left to right, histogram of deviance residuals, deviance residual cloud, and quantile-quantile plot.	19
11	Top panel: Fit of the generalized depletion model to the Ecuadorian artisanal fleet catch data (top panel), with target symbols indicating the timing of annual recruitment. The catch is the total catch by all fleets in the last year, and the biomass is the biomass at the last month of the times series (December 2019). Bottom panels: from left to right, histogram of deviance residuals, deviance residual cloud, and quantile-quantile plot.	21
12	Top panel: Fit of the generalized depletion model to the Ecuadorian fibreglass fleet catch data (top panel), with target symbols indicating the timing of annual recruitment. The catch is the total catch by all fleets in the last year, and the biomass is the biomass at the last month of the times series (December 2019). Bottom panels: from left to right, histogram of deviance residuals, deviance residual cloud, and quantile-quantile plot.	23
13	Top panel: Aggregate exploitation rate for each fleet and in total. Middle panel: instantaneous exploitation rate per fleet and in total. Bottom panel: stock biomass and catch in weight.	25
14	Pairwise correlations between parameter estimates (including 3 or four parameters in Pella-Tomlinson and 33 annual biomass predictions) and model selection criteria of sixteen hypotheses for the biomass population dynamics of the dolphinfish stock in the South-Eastern Pacific. Single regime (top left panels) are null hypothesis models with no influence of environmental cycles. Two regimes are hypotheses that involve changes in K , p or r singly, or in pairs or the trio of parameters of Pella-Tomlinson surplus production model. Panels with a green border are the best working models.	27
15	November stock biomass estimated by the best generalized depletion model in the extended CatDyn software (variant 36), best Pella-Tomlinson model of population dynamics (variant 4b), and total annual catch by four fleets operating in the dolphinfish fishery in the South-Eastern Pacific.	28

List of Tables

1	Directly estimated parameters corresponding to the Peruvian artisanal fleet of the best generalized depletion model (variant 36) fitted the 192 months (2004 to 2019) of effort and catch data of the the dolphinfish fishery in the South-East Pacific. Variant 36 was fitted with the adjusted profile normal distribution for all four fleets, the CG numerical algorithm, recruitment timings as suggested by the catch spike statistic with a few adjustments. MLE: maximum likelihood estimate. CV: coefficient of variation. CVs not shown correspond to optimization failures for second order properties at particular parameters.	18
2	Directly estimated parameters corresponding to the Peruvian fibreglass fleet of best generalized depletion model fitted (variant 36) the 192 months (2004 to 2019) of effort and catch data of the the dolphinfish fishery in the South-East Pacific. MLE: maximum likelihood estimate. Variant 36 was fitted with the adjusted profile normal distribution for all four fleets, the CG numerical algorithm, recruitment timings as suggested by the catch spike statistic with a few adjustments. CV: coefficient of variation. CVs not shown correspond to optimization failures for second order properties at particular parameters.	20
3	Directly estimated parameters corresponding to the Ecuadorian artisanal fleet of best generalized depletion model fitted (variant 36) the 192 months (2004 to 2019) of effort and catch data of the the dolphinfish fishery in the South-East Pacific. MLE: maximum likelihood estimate. Variant 36 was fitted with the adjusted profile normal distribution for all four fleets, the CG numerical algorithm, recruitment timings as suggested by the catch spike statistic with a few adjustments. CV: coefficient of variation. CVs not shown correspond to optimization failures for second order properties at particular parameters.	22
4	Directly estimated parameters corresponding to the Ecuadorian fibreglass fleet of best generalized depletion model fitted (variant 36) the 192 months (2004 to 2019) of effort and catch data of the the dolphinfish fishery in the South-East Pacific. Variant 36 was fitted with the adjusted profile normal distribution for all four fleets, the CG numerical algorithm, recruitment timings as suggested by the catch spike statistic with a few adjustments. MLE: maximum likelihood estimate. CV: coefficient of variation. CVs not shown correspond to optimization failures for second order properties at particular parameters.	24
5	Directly estimated parameters from the best Pella-Tomlinson model (B_0, K, r_1, r_2, p) and derived biological reference points ($MSY_1, MSY_2, B_{MSY}, \dot{P}_1, \dot{P}_2$) for the dolphinfish in the South-East Pacific according to parameterization in Eqs. 4, 6-8, likelihood model in Eq. 5. \dot{P}_1 and \dot{P}_2 are the annually averaged total latent productivity under the cold and warm environmental regimes, respectively (see Eq. 5). Mean catches during cold and warm periods are calculated within the 2004 to 2019 interval of years. B_{MSY} does not change from the cold to the warm periods of the environmental cycle because B_{MSY} does not depend on r (see Eq. 7).	29

References

- [1] B. Palko, G. Beardsley, and W. Richards, “Synopsis of the biological data on dolphin-fishes, *Coryphaena hippurus* linnaeus and *Coryphaena equiselis* linnaeus,” *NOAA Tech. Rep. NMFS Circ.*, vol. 443, pp. 1–28, 1982.
- [2] FAO, “The state of world fisheries and aquaculture 2020. sustainability in action,” tech. rep., Food and Agriculture Organization of the United Nations, 2020.
- [3] R. Mahon and H. Oxenford, “Precautionary assessment and management of dolphinfish in the Caribbean,” *Scientia Marina*, vol. 63, pp. 429–438, 1999.
- [4] K. Schwenke and J. Buckel, “Age, growth, and reproduction of dolphinfish (*Coryphaena hippurus*) caught off the coast of North Carolina,” *Fishery Bulletin (U.S.)*, vol. 59, pp. 82–92, 2008.
- [5] D. Benjamin and B. Kurup, “Stock assessment of dolphinfish, *Coryphaena hippurus* (linnaeus, 1758) off southwest coast of India,” *J. Mar. Biol. Ass. India*, vol. 54, pp. 95–99, 2012.
- [6] A. Baset, T. Haneef, A. Waris, B. Liao, A. Memon, E. Karim, and M. Ismail, “Maximum sustainable yield of dolphinfish, *Coryphaena hippurus* (linnaeus, 1758) fishery in Pakistan,” *Journal of Animal Science and Research*, vol. 2, pp. 1–5, 2020.
- [7] D. Hoggarth, S. Abeyasekera, R. Arthur, J. Beddington, R. Burn, A. Halls, G. Kirkwood, M. McAllister, P. Medley, C. Mees, G. Parkes, G. Pilling, R. Wakeford, and R. Welcomme, “Stock assessment for fishery management,” Tech. Rep. FAO Fisheries Technical Paper 487, FAO, Rome, 2006.
- [8] A. A. da Silva, J. Valero, M. Maunder, C. Minte-Vera, C. Lennert-Cody, M. Román, J. Martínez-Ortiz, E. Torrejón-Magallanes, and M. Carranza, “Exploratory stock assessment of dorado (*Coryphaena hippurus*) in the southeastern pacific ocean,” Tech. Rep. DOCUMENT SAC-07-06a(i), INTER-AMERICAN TROPICAL TUNA COMMISSION, 2016.
- [9] R. Methot and C. Wetzel, “Stock synthesis: A biological and statistical framework for fish stock assessment and fishery management,” *Fisheries Research*, vol. 142, pp. 86–99, 2013.
- [10] F.-C. II, “Report of the CopeMed II-MedSudMed workshop on the status of *Coryphaena hippurus* fisheries in the Western-Central Mediterranean, Cádiz, Spain, 8-9 october 2019,” Tech. Rep. FAO Technical Document 54, FAO GCP/INT/028/SPA-GCP/INT/362/EC, 2019.
- [11] V. Moltó, P. Hernández, M. Sinopoli, B. Benseddik, R. Besbes, A. Mariani, M. Gambin, F. Alemany, B. Morales-Nin, A. Grau, J. C. nas, J. Báez, M. Vasconcellos, L. Ceriola, and I. Catalán, “A global review on the biology of the dolphinfish (*Coryphaena hippurus*)

- and its fishery in the mediterranean sea: Advances in the last two decades,” *Reviews in Fisheries Science & Aquaculture*, vol. 28, pp. 376–420, 2020.
- [12] R. H. Roa-Ureta, “Modeling in-season pulses of recruitment and hyperstability-hyperdepletion in the *Loligo gahi* fishery of the Falkland Islands with generalized depletion models,” *ICES Journal of Marine Science*, vol. 69, pp. 1403–1415, 2012.
- [13] R. H. Roa-Ureta, “Stock assessment of the Spanish mackerel (*Scomberomorus commerson*) in Saudi waters of the Arabian Gulf with generalized depletion models under data-limited conditions,” *Fisheries Research*, vol. 171, pp. 68–77, 2015.
- [14] R. H. Roa-Ureta, C. Molinet, N. Barahona, and P. Araya, “Hierarchical statistical framework to combine generalized depletion models and biomass dynamic models in the stock assessment of the Chilean sea urchin (*Loxechinus albus*) fishery,” *Fisheries Research*, vol. 171, pp. 59–67, 2015.
- [15] Y.-J. Lin, W.-N. Tzeng, Y.-S. Han, and R. H. Roa-Ureta, “A stock assessment model for transit stock fisheries with explicit immigration and emigration dynamics: application to upstream waves of glass eels,” *Fisheries Research*, vol. 195, pp. 134–140, 2017.
- [16] R. H. Roa-Ureta, M. N. Santos, and F. L. ao, “Modelling long-term fisheries data to resolve the attraction versus production dilemma of artificial reefs,” *Ecological Modelling*, vol. 407, p. 108727, 2019.
- [17] R. H. Roa-Ureta, J. Henr quez, and C. Molinet, “Achieving sustainable exploitation through co-management in three chilean small-scale fisheries,” *Fisheries Research*, vol. 230, p. 105674, 2020.
- [18] R. H. Roa-Ureta, *CatDyn: Fishery Stock Assessment by Generalized Depletion Models*, 2015. R package version 1.1-1.
- [19] Scientific Advisory Committee on Fisheries, “Working group on stock assessment of small pelagic species (WGSASP),” tech. rep., FAO General Fisheries Commission for the Mediterranean, 2021.
- [20] V. Molt , I. Catal n, A. Ospina- lvarez, P. Hern ndez, and R. H. Roa-Ureta, “A multiannual five-fleet generalized depletion model for the stock assessment of the mediterranean dolphinfish (*Coryphaena hippurus*) fishery,” *ICES Journal of Marine Science*, vol. 79, pp. 1481–1496, 2022.
- [21] A. A. da Silva, C. Lennert-Cody, M. Maunder, M. Rom n-Verdesoto, C. Minte-Vera, N. Vogel, J. Mart nez-Ortiz, J. Carvajal, P. Guerrero, and F. Sondheimer, “Preliminary results from IATTC collaborative research activities on dorado in the eastern pacific ocean and future research plan,” Tech. Rep. DOCUMENT SAC-05-11b, INTER-AMERICAN TROPICAL TUNA COMMISSION, 2014.
- [22] S. Yang, Z. Li, J.-Y. YU, X. Hu, W. Dong, and S. He, “El ni o southern oscillation and its impact in the changing climate,” *National Science Review*, vol. 5, pp. 840–857, 2018.

-
- [23] T. Berger and F. Sibeni and F. Calderini, *FishStatJ*.
- [24] R Core Team, *R: A Language and Environment for Statistical Computing*. R Foundation for Statistical Computing, Vienna, Austria, 2020.
- [25] R. C. Team, “R: A language and environment for statistical computing.” <https://www.R-project.org/>, 2021.
- [26] S. van Buuren and K. Groothuis-Oudshoorn, “mice: Multivariate imputation by chained equations in r,” *Journal of Statistical Software*, vol. 45, no. 3, pp. 1–67, 2011.
- [27] M. Zuniga-Flores, *Dinámica poblacional del dorado (Coryphaena hippurus) en Baja California sur, México: implicaciones para su manejo*. PhD thesis, Instituto Politécnico Nacional, La Paz, México, 2009.
- [28] R. H. Roa-Ureta, M. del Pino Fernández-Rueda, J. L. A. na, A. Rivera, R. González-Gil, and L. García-Flórez, “Estimation of the spawning stock and recruitment relationship of *Octopus vulgaris* in asturias (bay of biscay) with generalized depletion models: implications for the applicability of msy,” *ICES Journal of Marine Science*, p. fsab113, 2021.
- [29] F. Maynou, “Application of a multi-annual generalized depletion model to the assessment of a data-limited coastal fishery in the western mediterranean,” *Scientia Marina*, vol. 79, pp. 157–168, 2015.
- [30] F. Maynou, M. Demestre, P. Martín, and P. Sánchez, “Application of a multi-annual generalized depletion model to the mediterranean sandeel fishery in catalonia,” *Fisheries Research*, vol. 234, p. 105814, 2021.
- [31] B. Meissa, M. Dia, B. C. Baye, M. Bouzouma, E. Beibou, and R. H. Roa-Ureta, “A comparison of three data-poor stock assessment methods for the pink spiny lobster fishery in mauritania,” *Frontiers in Marine Science*, vol. 8, p. 714250, 2021.
- [32] J. Nash and R. Varadhan, “Unifying optimization algorithms to aid software system users: optimx for r,” *Journal of Statistical Software*, vol. 43, pp. 1–14, 2011.
- [33] H.-H. Lee, M. Maunder, K. Piner, and R. Methot, “Estimating natural mortality within a fisheries stock assessment model: An evaluation using simulation analysis based on twelve stock assessments,” *Fisheries Research*, vol. 109, pp. 89–94, 2011.
- [34] S. Anderson, C. Monnahan, K. Johnson, K. Ono, and J. Valero, “ss3sim: An r package for fisheries stock assessment simulation with stock synthesis,” *PLoS ONE*, vol. 9(4), p. e92725, 2014.
- [35] F. Hurtado-Ferro, C. Szuwalski, J. Valero, S. Anderson, C. Cunningham, K. Johnson, R. Licandeo, C. McGilliard, C. Monnahan, M. Muradian, K. Ono, K. Vert-Pre, A. Whitten, and A. Punt, “Looking in the rear-view mirror: bias and retrospective patterns in integrated, age-structured stock assessment models,” *ICES Journal of Marine Science*, vol. 72, pp. 99–110, 2015.
-

-
- [36] J. Thorson, A. Hicks, and R. Methot, “Random effect estimation of time-varying factors in stock synthesis,” *ICES Journal of Marine Science*, vol. 72, pp. 178–185, 2015.
- [37] K. Patterson, “Fisheries for small pelagic species: an empirical approach to management targets,” *Reviews in Fish Biology and Fisheries*, vol. 2, pp. 321–338, 1992.
- [38] C. Wang, “A review of ENSO theories,” *National Science Review*, vol. 5, pp. 813–825, 2018.
- [39] R. D. T.J. Quinn II, *Quantitative Fish Dynamics*. New York: Oxford University Press, 1999.
- [40] D. Fournier, J. Skaug, J. Ancheta, J. Ianelli, A. Magnusson, and M. Maunder, “Ad model builder: using automatic differentiation for statistical inference of highly parameterized complex nonlinear models,” *Optimization Methods and Software*, vol. 27, pp. 233–249, 2012.
- [41] A. Magnusson, *ADMB-IDE: Easy and efficient user interface*. ADMB Foundation, 2009.